CDK11 facilitates centromeric transcription to maintain centromeric cohesion during mitosis

Qian Zhang[a], Yujue Chen[a], Zhen Teng[a], Zhen Lin[b,d], and Hong Liu[a,b,c,*]
[a]Department of Biochemistry and Molecular Biology, [b]Tulane Cancer Center, [c]Tulane Aging Center, and [d]Department of Pathology and Laboratory Medicine, Tulane University School of Medicine, New Orleans, LA 70112

ABSTRACT **Actively-transcribing RNA polymerase (RNAP)II is remained on centromeres to maintain centromeric cohesion during mitosis, although it is largely released from chromosome arms. This pool of RNAPII plays an important role in centromere functions. However, the mechanism of RNAPII retention on mitotic centromeres is poorly understood. We here demonstrate that Cyclin-dependent kinase (Cdk)11 is involved in RNAPII regulation on mitotic centromeres. Consistently, we show that Cdk11 knockdown induces centromeric cohesion defects and decreases Bub1 on kinetochores, but the centromeric cohesion defects are partially attributed to Bub1. Furthermore, Cdk11 knockdown and the expression of its kinase-dead version significantly reduce both RNAPII and elongating RNAPII (pSer2) levels on centromeres and decrease centromeric transcription. Importantly, the overexpression of centromeric α-satellite RNAs fully rescues Cdk11-knockdown defects. These results suggest that the maintenance of centromeric cohesion requires Cdk11-facilitated centromeric transcription. Mechanistically, Cdk11 localizes on centromeres where it binds and phosphorylates RNAPII to promote transcription. Remarkably, mitosis-specific degradation of G2/M Cdk11-p58 recapitulates Cdk11-knockdown defects. Altogether, our findings establish Cdk11 as an important regulator of centromeric transcription and as part of the mechanism for retaining RNAPII on centromeres during mitosis.**

Monitoring Editor
Rong Li
Johns Hopkins University and National University of Singapore

Received: Aug 7, 2023
Revised: Nov 20, 2023
Accepted: Nov 21, 2023

New Hypothesis

SIGNIFICANCE STATEMENT

- RNAPII localizes to the centromere to promote its function, but how RNAPII is regulated at centromeres is poorly understood.
- We hereby identify Cdk11 as part of the mechanism to maintain centromeric RNAPII during mitosis.
- This finding uncovers a new mechanism controlling proper chromosome segregation.

This article was published online ahead of print in MBoC in Press (http://www.molbiolcell.org/cgi/doi/10.1091/mbc.E23-08-0303) on November 29, 2023.

Conflict of interests: The authors declare no competing financial interests.

Author contributions: Conceptualization, Funding acquisition, Resources and Supervision: H. Liu; Methodology: Q. Zhang, Y.J. Chen, Z. Teng, Z. Lin, and H. Liu; Investigation: Q. Zhang, Y.J. Chen, and Z. Teng; Writing-original draft: Q. Zhang and H. Liu; Writing-review and editing: Q. Zhang, Y.J. Chen, Z. Teng, and H. Liu.

*Address correspondence to: Hong Liu (hliu22@tulane.edu).

Abbreviations used: Cdk11, Cyclin-dependent kinase 11; RNAPII, RNA polymerase II; Sgo1, Shugoshin 1.

INTRODUCTION

The noncoding centromere, a specialized region of a chromosome, dictates the assembly of kinetochore that is essential for proper chromosome segregation during mitosis. Such a critical centromere function is conserved across eukaryotes and is determined by the centromere-specific histone H3 variant CENP-A (McKinley and Cheeseman, 2016). Proper incorporation of CENP-A into centromeric chromatin is prerequisite for CENP-A to fulfill its duty. Unlike canonical histones that are usually incorporated into chromatin in a DNA duplication-dependent manner during S phase, newly synthesized CENP-A is instead deposited into centromeric chromatin independently of DNA replication mainly during G1 phase (Jansen *et al.*, 2007; Schuh *et al.*, 2007). This process requires RNA polymerase

(RNAP)II-catalyzed transcription (Bobkov *et al.*, 2018; Bury *et al.*, 2020), suggestive of an essential role of centromeric transcription in centromere functions. In addition to in interphase, centromeric transcription is also undergoing during mitosis (Chan *et al.*, 2012; Liu *et al.*, 2015; Bobkov *et al.*, 2018; Perea-Resa *et al.*, 2020; Chen *et al.*, 2021). The ongoing centromeric transcription facilitates the installment of an essential cohesion-protector Sgo1 onto centromeres to protect centromeric cohesion during mitosis in human cells (Liu *et al.*, 2015; Chen *et al.*, 2021). Thus, centromeric transcription plays diverse critical roles in regulating centromere functions and chromosome segregation (Talbert and Henikoff, 2018).

As such, how centromeric transcription is regulated is poorly understood. In budding yeast, centromere-binding factor cbf1 and histone H2A variant Htz1 have been demonstrated to repress centromeric transcription (Ling and Yuen, 2019). In human cells, the nucleolus and ZFAT was suggested to regulate centromeric transcription as well (Bury *et al.*, 2020; Ishikura *et al.*, 2020). Thus, there exist factors that may be more specific for centromeric transcription. Identification of these factors would be a great help of understanding the regulation of centromeric transcription. When cells enter mitosis, RNAPII and its associated factors are largely released from chromosomes, thus leading to a global suppression for transcription (Parsons and Spencer, 1997; Palozola *et al.*, 2018; Teves *et al.*, 2018). However, a pool of RNAPII is remained on mitotic centromeres to actively transcribe centromeres (Chan *et al.*, 2012; Liu *et al.*, 2015; Bobkov *et al.*, 2018; Perea-Resa *et al.*, 2020; Chen *et al.*, 2021). Therefore, a mechanism must exist to maintain active RNAPII on centromeres during mitosis. Identification of the factors specific to centromeric transcription during mitosis would help resolve such a mechanism.

Cdk11 belongs to the cyclin-dependent kinase family, which contains several members that are important for transcriptional regulation, including Cdk7 and Cdk9 (Chou *et al.*, 2020). These kinases phosphorylate either RNAPII at Ser5 to facilitate transcriptional initiation or RNAPII at Ser2 to promote transcriptional elongation, establishing these kinases as universal regulators for RNAPII gene transcription (Lu *et al.*, 1992; Serizawa *et al.*, 1995; Peng *et al.*, 1998; Fu *et al.*, 1999; Spangler *et al.*, 2001). Interestingly, extensive studies have suggested important roles of Cdk11 in transcriptional regulation. First, Cdk11 regulates mRNA splicing and processing (Loyer *et al.*, 1998; Dickinson *et al.*, 2002; Trembley *et al.*, 2002; Hu *et al.*, 2003; Loyer *et al.*, 2008; Valente *et al.*, 2009; Pak *et al.*, 2015; Hluchy *et al.*, 2022). Secondly, in fission yeast, Cdk11 has been shown to phosphorylate the transcriptional-mediator complex (Drogat *et al.*, 2012). In addition, Cdk11 can also directly phosphorylate the Ser2 of the RNAPII CTD to regulate HIV viral transcription (Pak *et al.*, 2015). More recently, Gajduskova *et al.* (2020) showed that Cdk11 promotes the transcription of replication-dependent histone (RDH) genes via phosphorylating Ser2 of the RNAPII CTD. These observations suggest that, unlike the universal transcriptional regulators Cdk7 and Cdk9, Cdk11 may function exclusively on a subset of genes to enhance their transcription, which might be important for some specific cellular needs. As such, it would be of interest to determine whether Cdk11 could also be important for the transcription of noncoding DNA sequences, such as centromeres. Several previous observations suggested that Cdk11 is involved in centromere regulation. Cdk11 knockout in mice resulted in early embryonic lethality due to apoptosis of the blastocyst cells (Li *et al.*, 2004). Cells within these embryos exhibited mitotic arrest (Li *et al.*, 2004). Cdk11 knockdown in human cells also caused increase in mitosis-arrested cells that suffered severe centromeric cohesion defects (Hu *et al.*, 2007; Rakkaa *et al.*, 2014). All these findings highlight the importance of Cdk11 in regulating centromeric cohesion. Interestingly, a Cdk11 isoform p58 is generated from an internal ribosomal site on Cdk11 mRNAs exclusively during G2/M phase (Xiang *et al.*, 1994; Cornelis *et al.*, 2000), suggesting a potential important role of Cdk11-p58 in mitotic regulation. Based on these observations, together with our findings that centromeric transcription facilitates centromeric cohesion, we thereby hypothesized that Cdk11 might promote centromeric transcription to maintain centromeric cohesion.

In this study, we address whether and how Cdk11 regulates centromeric transcription in human cells. Cdk11 knockdown significantly reduces RNAPII and RNAPII-pSer2 levels at centromeric chromatin, reduces centromeric transcription and weakens centromeric cohesion. Overexpression of centromeric a-satellite RNAs completely rescues Cdk11-knockdown phenotypes. Importantly, mitosis-specific degradation of G2/M Cdk11 p58 recapitulates Cdk11-knockdown defects. Thus, our findings establish Cdk11 as an important regulator of centromeric transcription as well as part of the mechanism for retaining RNAPII on centromeres during mitosis.

RESULTS

Cdk11 knockdown moderately decreases Bub1 recruitment to kinetochores

Cdk11 knockdown resulted in centromeric cohesion defects in mitosis and the defects had been attributed to decreased Bub1 recruitment to kinetochores (Hu *et al.*, 2007; Rakkaa *et al.*, 2014). To confirm the role of Bub1 in Cdk11-mediated centromeric cohesion, we reexamined Bub1 kinetochore localization in Cdk11-knockdown cells. We transfected HeLa Tet-On cells with luciferase (mock) or two distinct Cdk11 siRNA oligos (#1 and #6) and then collected mitotic cells for chromosome spread and immunostaining after brief nocodazole treatment. As a comparison, Bub1 siRNA oligos were also included. Western-blot analyses demonstrated that both Cdk11 siRNA oligos dramatically decreased the protein levels of Cdk11-p110 in log-phase cells and the ones of Cdk11-p110 and -p58 in mitosis (Figures 2F; Supplemental Figures S4, B and C). Consistently, Bub1 levels on kinetochores were decreased by more than 90% upon Bub1 knockdown, whereas Cdk11 knockdown only moderately reduced Bub1 levels by ~40% (Figures 1, A and B). Approximately 90% of Cdk11-knockdown cells exhibited impaired centromeric cohesion. Further analyses demonstrated a heterogeneity of Bub1 kinetochore localizations among these cells (Figure 1A). While Bub1 levels were reduced at kinetochores in 47% of cells after Cdk11 knockdown, 32% of Cdk11-knockdown cells still showed strong Bub1 signals with weakened centromeric cohesion and 11% of Cdk11-knockdown cells showed strong Bub1 signals with severely impaired centromeric cohesion (Figure 1A). Importantly, with such a milder decrease in Bub1 levels on kinetochores, Cdk11 knockdown even induced more severe centromeric cohesion defects than Bub1 knockdown, revealed by the increased sister-centromeres distance (Figure 1, B and C). These results strongly suggest that other factors beyond Bub1 also contribute to Cdk11-regulated centromeric cohesion. Bub1 recruitment to kinetochores is dependent on the Mps1 phosphorylation of Knl1 MELT domains (Primorac *et al.*, 2013; Zhang *et al.*, 2014). To further understand how Cdk11 knockdown decreased Bub1 recruitment to kinetochores, we analyzed Knl1 phospho-MELT levels on kinetochores in Cdk11-knockdown cells. We transfected HeLa Tet-On cells with luciferase (mock) or Cdk11 siRNAs and then collected them for chromosome spread and immunostaining after brief nocodazole treatment. Interestingly, Cdk11 knockdown decreased the levels of Knl1 phospho-MELT by ~40% (Figure 1, D and E) on kinetochores, likely explaining why Bub1 kinetochore recruitment is impaired in Cdk11-knockdown cells.

Bub1 enriches Sgo1 to centromeres during mitosis (Tang *et al.*, 2004; Kitajima *et al.*, 2005; Kawashima *et al.*, 2010). If Bub1 decrease from kinetochores was responsible for Cdk11-knockdown–induced centromeric cohesion defects, Sgo1 would also be expected to decrease from centromeres. We transfected HeLa Tet-On cells with luciferase (mock) or Cdk11 siRNAs and then collected mitotic cells for chromosome spread and immunostaining after brief nocodazole treatment. In more than 80% of nocodazole-arrested mock-treated HeLa Tet-On cells, Sgo1 localized to inner centromeres with robust centromeric cohesion (Figure 1, F and G). In contrast, three types of Sgo1 localization patterns were observed in nocodazole-arrested Cdk11-knockdown cells: strong inner-centromeric Sgo1 localization with normal centromeric cohesion (type I, ~20%), reduced centromeric Sgo1 localization with weakened centromeric cohesion (type II, ~35%), and robust centromeric Sgo1 localization with weakened centromeric cohesion (type III, ~45%). Again, Heterogeneity of Sgo1 localizations on kinetochores in Cdk11-knockdown cells was observed, like Bub1. Thus, other pathway(s) beyond the Bub1-Sgo1 pathway may also contribute to Cdk11-regulated centromeric cohesion.

Ectopic targeting of Bub1 to kinetochores partially rescues centromeric cohesion defects upon Cdk11 knockdown

To further assess to what extent Bub1 contributes to Cdk11-mediated centromeric cohesion, we decided to target Bub1 to kinetochores by fusing it with kinetochore protein Mis12. Functionality of this fusion protein Mis12-Bub1 was firstly examined. We transfected HeLa Tet-On cells with Bub1 siRNAs and plasmids containing GFP-Mis12-Bub1 (kinase domain, resides: 633-1085) WT or kinase dead (KD). After brief nocodazole treatment, we collected mitotic cells for chromosome spread followed by immunostaining to examine Sgo1 localization. Consistent with the previous findings (Tang *et al.*, 2004; Kitajima *et al.*, 2005; Liu *et al.*, 2013; Williams *et al.*, 2017), Bub1 knockdown dramatically decreased Sgo1 levels from centromeres (Figure 2, A and B, upper panel; Supplemental Figure S1A). Expression of GFP-Mis12-Bub1 WT, not KD, completely restored Sgo1 levels in Bub1-knockdown cells (Figure 2, A and B, upper panel; Supplemental Figure S1A) albeit they both localized to kinetochores similarly (Figure 2B, lower panel). Thus, Mis12 can effectively target fully functional Bub1 to kinetochores. We next examined the extent to which these fusion proteins rescued the phenotypes of Cdk11 knockdown. Consistently, Cdk11 knockdown moderately decreased Sgo1 localization on centromeres and significantly weakened centromeric cohesion (Figure 2, C and D; Supplemental Figure S1C). Expression of GFP-Mis12-Bub1 WT, not KD, fully restored centromeric Sgo1 levels but only partially rescued the centromeric cohesion defects (Figure 2D; Supplemental Figure S1C). Detailed analyses revealed that expression of WT only reduced the number of type II cells (from ~20 to ~5%), but barely affected type III cells (from ~45 to ~48%; Figure 2E). These results further confirm that the Bub1-Sgo1 pathway partially contributes to Cdk11-regulated centromeric cohesion. Other unknown mechanisms are yet to be uncovered.

Cdk11 is an important regulator of mRNA splicing and processing (Loyer *et al.*, 1998; Dickinson *et al.*, 2002; Trembley *et al.*, 2002; Hu *et al.*, 2003; Loyer *et al.*, 2008; Valente *et al.*, 2009). Defective mRNA splicing has been shown to decrease the protein levels of an essential cohesion protector Sororin, leading to centromeric cohesion defects (Oka *et al.*, 2014; Sundaramoorthy *et al.*, 2014; van der Lelij *et al.*, 2014; Watrin *et al.*, 2014). We therefore examined whether Cdk11-knockdown–induced centromeric cohesion defects were a consequence of reduced protein levels of Sororin and/or other cohesion regulators. Western-blot analyses demonstrated that none of Smc1, Bub1, Sgo1, and Sororin protein levels was significantly changed in Cdk11-knockdown cells (Figure 2F). Thus, cohesin and the critical cohesion regulators are unlikely involved in Cdk11-regulated centromeric cohesion regulation. However, we cannot completely exclude the possibility that Cdk11-mediated mRNA splicing of other factors contributes to the maintenance of centromeric cohesion.

Cdk11 and its kinase activity maintain RNAPII and RNAPII-pSer2 on centromeres in both mitosis and interphase

Centromeric transcription maintains centromeric cohesion and Cdk11 is a transcription regulator (Loyer and Trembley, 2020; Chen *et al.*, 2021). We therefore hypothesized that in addition to promoting Bub1, Cdk11 facilitates centromeric transcription to maintain centromeric cohesion. To test this hypothesis, we first examined how Cdk11 regulates RNAPII and elongating RNAPII (pSer2) as RNAPII is enriched at human centromeres during mitosis (Chan *et al.*, 2012; Liu *et al.*, 2015; Perea-Resa *et al.*, 2020; Chen *et al.*, 2021). We transfected HeLa Tet-On cells with luciferase (mock) or distinct Cdk11 siRNAs. After brief nocodazole treatment, we collected mitotic cells for chromosome spread and immunostaining. Two different types of RNAPII antibodies were used to recognize total (4H8) and phospho-Ser2 (H5) of RNAPII on centromeres (Chan *et al.*, 2012; Liu *et al.*, 2015; Chen *et al.*, 2021). Consistently, robust RNAPII and RNAPII-pSer2 signals were detected in mock centromeres (Figure 3, A and E). Encouragingly, Cdk11 knockdown by two distinct siRNAs largely decreased both RNAPII and RNAPII-pSer2 signals on centromeres (Figure 3, B and F); at the same time, these cells suffered centromeric cohesion defects (Figure 3G). Decreased RNAPII-pSer2 levels and weakened centromeric cohesion were also observed in nocodazole-arrested mitotic nontransformed RPE1 cells of Cdk11 knockdown, suggesting that Cdk11-knockdown–caused phenotypes are not cell type-specific (Figure 3, C and D; Supplemental Figure S2A). In addition, using chromatin immunoprecipitation (ChIP), we found that Cdk11 knockdown decreased RNAPII-pSer2 levels on centromeres, but did not do so on two intergenetic regions in log-phase HeLa Tet-On cells (Figure 3I; Supplemental Figure S2C). Thus, Cdk11 promotes RNAPII association with centromeres in both mitosis and interphase.

We next determined whether Cdk11 kinase activity is required for RNAPII localization on centromeres. As our siRNA oligos knocked down two major isoforms (p110 and p58; Supplemental Figure S4, B and C), we examined RNAPII levels on centromeres in cells expressing either transgenic Cdk11-p110 or -P58 after Cdk11 knockdown. We knocked down endogenous Cdk11 in HeLa Tet-On cells stably expressing Myc-Cdk11-p110 WT or KD mutant, and then then harvested mitotic cells for chromosome spread and immunostaining after brief nocodazole treatment. Western blot analyses showed that Myc-Cdk11-p110 WT and KD were expressed at a comparable level in Cdk11-knockdown cells (Figure 3H). Expression of Myc-Cdk11-p110 WT completely restored RNAPII levels on centromeres, but Cdk11-p110 KD failed to do so (Figure 3, E and F), suggesting that the Cdk11-p110 kinase activity is required for the centromeric localization of RNAPII. Accordingly, expression of Cdk11-p110 WT, not KD, also completely rescued centromeric cohesion defects and Sgo1 levels (Figure 3, E and F; Supplemental Figure S2B). We then examined the effect of Cdk11-p58 on centromeric RNAP II, an isoform that is specifically expressed at G2/M phase and plays an essential role in protecting centromeric cohesion during mitosis (Hu *et al.*, 2007; Rakkaa *et al.*, 2014). We transfected HeLa Tet-on cells with endogenous Cdk11 knockdown with vector, myc-Cdk11-p58 WT, or KD mutant, and collected cells for

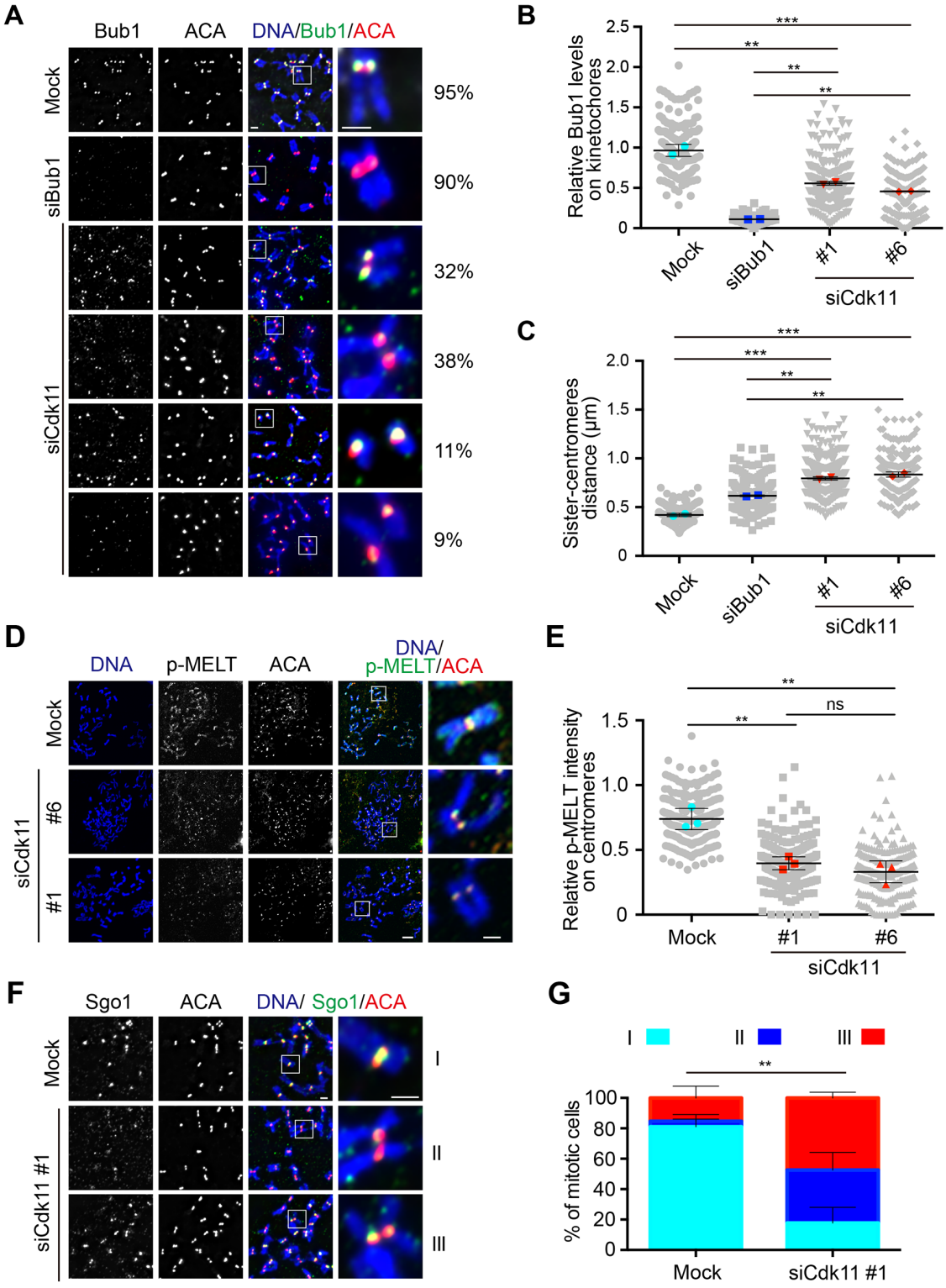

FIGURE 1: Cdk11 knockdown partially decreases Bub1 and Knl1 p-MELT levels on kinetochores. (A) Bub1 levels on kinetochores are moderately reduced by Cdk11 knockdown. Nocodazole-arrested HeLa Tet-On cells were transfected with luciferase (mock), Bub1 or Cdk11 (#1 and #6) siRNAs and then subjected to chromosome spread and immunostaining with the indicated antibodies. Heterogeneity of Bub1 localizations on kinetochores in Cdk11-knockdown cells was observed. Percentage of each type of Bub1 localization patterns is shown in the right panel: strong kinetochore Bub1 localization with weakened centromeric cohesion (32%), reduced kinetochore Bub1 localization with weakened centromeric cohesion (38%), strong kinetochore Bub1 localization with severely impaired centromeric cohesion (11%), and reduced kinetochore Bub1 localization with severely impaired centromeric cohesion (9%). Scale bars, 5 μm and 1 μm, respectively. (B and C) Quantifications of relative Bub1 levels (Bub1/ACA, B) and the distance of inter-sister centromeres (C) in (A). These quantifications were performed based on two independent experiments. In total, 195, 117, 236, and

chromosome spread and immunostaining after brief nocodazole treatment. Similarly, Cdk11-p58 WT completely restored RNAPII levels and centromeric cohesion defects in Cdk11-knockdown cells, but KD failed to do so (Supplemental Figure S3, A–D). These results suggest that either Cdk11-p110 activity or -p58 activity is sufficient for RNAPII retention on centromeres during mitosis. Cdk11-p110 or -p58 may collaborate to maintain RNAP II on centromeres.

Mitosis-specific degradation of Cdk11 results in centromeric cohesion defects and dislodges RNAPII from centromeres

As Cdk11 is also required for maintaining RNAPII on centromeres in interphase, reduced RNAPII levels on centromeres in mitosis could be a legacy inherited from interphase. Therefore, we sought to determine whether mitotic Cdk11 is required for maintaining RNAPII on centromeres and to examine centromeric cohesion during mitosis by mitosis-specifically degrading G2/M Cdk11-p58. We transfected HeLa Tet-On cells stably expressing the auxin (indole-3 acid, IAA) receptor Myc-TiR1 with siCdk11 and GFP-AID-Cdk11-p58, and then treated cells with nocodazole. Nocodazole-arrested mitotic cells were harvested and further treated with IAA for 3 h (Figure 4A). Western blot analyses demonstrated that GFP-AID-Cdk11-p58 protein levels were largely degraded 3 h after auxin treatment (Figure 4B), validating this system. Consistently, expression of GFP-AID-Cdk11-p58 completely rescued the reduced RNAPII levels on centromeres and centromeric cohesion defects in Cdk11-knockdown cells (Figure 4, C–E). Strikingly, degradation of GFP-AID-Cdk11-p58 by IAA treatment recapitulated the defects by Cdk11 knockdown, thus supporting that mitotic Cdk11 is required for maintaining centromeric RNAPII and centromeric cohesion during mitosis.

As Cdk11 knockdown decreased centromeric RNAPII levels in mitosis, we reasoned that Cdk11 overexpression could increase them. To test this, we examined centromeric RNAPII in nocodazole-arrested HeLa Tet-On cells stably expressing Myc-Cdk11-p110 or -p58. As expected, expression of both isoforms of Cdk11 augmented RNAPII signals on centromeres (Figure 4, F and G; Supplemental Figure S4D). Surprisingly, an increase of ectopic RNAPII on chromosome arms was also observed in some of Cdk11-p58 cells (Figure 4H), likely due to its overexpression (Supplemental Figure S4A)

Cdk11 localizes to chromatin including centromeres in both mitosis and interphase

We next sought to determine whether Cdk11 could localize to centromeres as it regulates centromeric RNAPII. We performed chromosome spread followed by immunostaining in nocodazole-arrested HeLa Tet-On cells. As shown in Figure 5A, Cdk11 signals, validated by Cdk11 knockdown, were detected along the entire length of mitotic chromosomes with a slight enrichment on some centromeres (Figure 5, A and B;Supplemental Figure S4E), which supports a direct role of Cdk11 in regulating centromere transcription. Because expression of either Cdk11-p110 or -p58 could rescue centromeric cohesion defects and reduced centromeric RNAPII levels in Cdk11-knockdown cells, we speculated that both isoforms could localize on centromeres for their functions. To test this, we examined Cdk11 localization in Cdk11 knockdown Hela Tet-on cells stably expressing Cdk11-p110 or -p58 and found that the expression of either Cdk11-p110 or -p58 completely restored Cdk11 levels on centromeres as well as chromosome arms in Cdk11-knockdown cells (Figure 5, C–E). At the same time, reduced RNAPII levels were also rescued upon expression of Cdk11-p110 or -p58 (Figure 5D), suggestive of a critical role of Cdk11 in maintaining RNAPII on centromeres. These results also suggest that centromere-localized Cdk11-p110 and -p58 likely play a similar role in retaining active RNAPII for centromeric cohesion maintenance in mitosis. Noticeably, Cdk11 was often found to localize to chromosome arms, indicating that Cdk11-regulated RNAPII may not be specific to centromeres. In the future, it will be of our interest to determine why centromeric pool, not chromosome-arm pool of Cdk11 supports active RNAPII transcription during mitosis.

To determine whether Cdk11 is also localized on centromeres in interphase, we performed ChIP to detect the presence of Cdk11-p110 on centromeres. As shown in Figure 5F, Myc-Cdk11 was detected at both the tested gene regions, including RDH genes (Gajduskova *et al.*, 2020), and centromeres, suggesting that Cdk11 can localize to centromeres in interphase cells albeit its localization may not be specific to centromeres. Taken all the results together, Cdk11 localizes on centromeres in both mitosis and interphase.

142 centromeres were scored for mock, siBub1, siCdk11 #1, and siCdk11 #6, respectively, in (B); 320, 210, 360, and 225 sister-centromere pairs were scored for mock, siBub1, siCdk11 #1 and siCdk11 #6, respectively, in (C) The pooled data is grey-coded. The mean calculated from each biological replicate is color-coded. The average and SD calculated from means of two biological replicates are shown here. Differences were assessed using ANOVA followed by pairwise comparisons using Tukey's test. Two-tailed test were used. Quantification details hereafter were recorded in the section of *Materials and Methods*. (D) Knl1 p-MELT levels on kinetochores are reduced by Cdk11 knockdown. Nocodazole-arrested HeLa Tet-On cells were transfected with luciferase (mock) and Cdk11 (#1 and #6) siRNAs and then subjected to chromosome spread and immunostaining with the indicated antibodies. Scale bars, 5 μm and 1 μm, respectively. (E) Quantification of relative p-MELT intensity (p-MELT/ACA) in (D). The quantification was performed based on three independent experiments. In total, 244, 234, and 228 centromeres were scored for mock, siCdk11 #1 and siCdk11 #6, respectively. The pooled data is grey-coded. The mean calculated from each biological replicate is color-coded. The average and SD calculated from means of three biological replicates are shown here. Differences were assessed using ANOVA followed by pairwise comparisons using Tukey's test. Two-tailed test were used. (F) Sgo1 localization in Cdk11-knockdown cells. Nocodazole-arrested HeLa Tet-On cells were transfected with luciferase (mock) or Cdk11 (#1) siRNAs and then subjected to chromosome spread and immunostaining with the indicated antibodies. Scale bars, 5 μm and 1 μm, respectively. (G) Quantification of Sgo1 localization patterns in Cdk11-knockdown cells. Three types of Sgo1 localization patterns were observed: strong inner-centromeric Sgo1 localization with normal centromeric cohesion (type I), reduced centromeric Sgo1 localization with weakened centromeric cohesion (type II), and robust centromeric Sgo1 localization with weakened centromeric cohesion (type III). In total, 167 and 124 cells were scored for mock and siCdk11 #1, respectively. The quantification was carried out based on three independent repeats. The average and SD calculated from at least three independent experiments are shown here. Differences were assessed using *t* test. Two-tailed test were used. ns denotes not significant; **, $P < 0.01$; ***, $P < 0.001$.

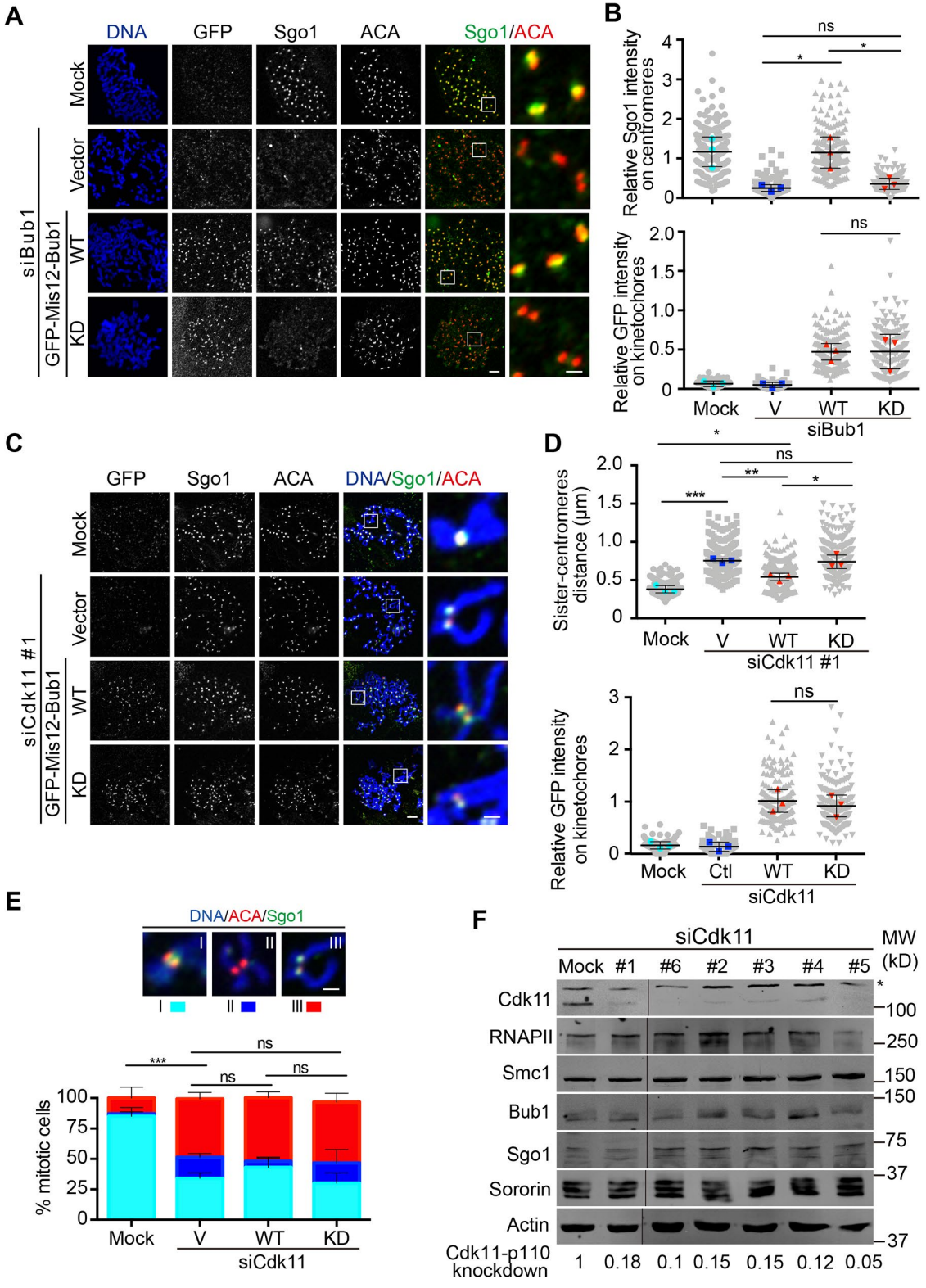

FIGURE 2: Ectopically targeting Bub1 to kinetochore partially relieves centromeric cohesion defects in Cdk11-knockdown cells. (A) Targeting Bub1 kinase domain to kinetochores by Mis12 fully rescues Sgo1 localization defects on kinetochores in Bub1-knockdown cells. HeLa Tet-On cells treated with luciferase (mock) or Bub1 siRNAs were transfected with vector or GFP-Mis12-Bub1 (631-1085) WT or KD (D946N). Cells were then treated with nocodazole for 2 h and mitotic cells were collected for chromosome spread and immunostaining with the indicated antibodies. Scale bars, 5 μm and 1 μm, respectively. (B) Quantifications of relative Sgo1 levels on centromeres (Sgo1/ACA, top panel) and GFP levels on kinetochores (GFP/ACA, bottom panel) in (A). These quantifications were performed based on three independent experiments. In total, 197, 188, 194, and 188 centromeres were scored for mock, siBub1, GFP-Mis12-Bub1 WT and KD, respectively. The pooled data is grey-coded. The mean calculated from each biological replicate is

Cdk11-p110 and -p58 both physically interact with RNAPII in cells

Cdk11-p110 was shown to bind the CTD of RNAPII in vivo (Trembley *et al*., 2003), and phosphorylate RNAPII at Ser2 (Gajduskova *et al*., 2020). We then examined whether the binding of Cdk11 with RNAPII is dependent on its kinase activity in cells. HeLa Tet-On cells stably expressing Myc-Cdk11-p110 WT or KD were cross-linked with formaldehyde and the resulting cell lysates were subjected to RNAPII immunoprecipitation (IP). As a result, both Myc-Cdk11-p110 WT and KD bound with RNAPII (Figure 6A), suggesting that the Cdk11-RNAPII binding is independent of Cdk11 kinase activity. We also found that Cdk11-p58 also physically interacted with RNAPII (Figure 6B). As Cdk11-p58 shares the same C-terminus with Cdk11, it is very likely that Cdk11 binds to RNAPII through its C-terminus.

Cdk11 knockdown or expression of its kinase-dead version decreases the levels of centromeric α-satellite RNAs

As Cdk11 is required for maintaining active RNAPII on centromeres, we then sought to determine how Cdk11 regulates centromeric α-satellite RNAs. We transfected different Cdk11 siRNAs into HeLa Tet-on cells and then extracted total RNAs for real-time PCR analysis using two gene primers (GAPDH and RPL30) and two centromeric α-satellite primers (α-Sat-4 and α-Sat-13/21). Although four distinct Cdk11 siRNA oligos had varying effects on the amounts of the tested mRNAs, slightly decreasing GAPDH and increasing RPL30, the amounts of centromeric α-satellite RNAs on Sat-4 and Sat-13/21 were unanimously reduced to varying levels (Figure 7A), suggesting that Cdk11 promotes centromeric transcription. To further confirm this, we also examined the effects of Cdk11 knockdown on centromeric α-satellite RNAs derived from other alpha-satellite higher-order repeats (HORs). Surprisingly, Cdk11 knockdown tended to decrease alpha-satellite HOR RNAs with lower CT values (D18Z1, D19Z5, and D21Z1), but not the ones with higher CT values (D1Z7, D8Z2, D16Z2, and D18Z2; Figure 7B), suggesting that centromeric regions with higher transcriptional activities are more prone to Cdk11 regulation. We next determined whether Cdk11 regulates transcriptional activity on centromeres by examining 5′-Ethynyl Uridine (EU)-labeled nascent RNA transcripts. We transfected HeLa Tet-on cells with Cdk11 siRNAs into and then chased with EU 1 h before harvest. EU-labeled RNAs were then purified and subjected to real-time PCR analysis. Consistently, Cdk11 knockdown only slightly affected the transcriptional activities on GAPDH and RPL30 genes (Figure 7C). In contrast, Cdk11 knockdown significantly reduced the transcriptional activities on the two tested centromeric regions. Neither gene nor centromeric transcription was affected by Bub1 knockdown in interphase cells. These results, together with its requirement in maintaining active RNAPII on centromeres, indicate that Cdk11 facilitates centromeric transcription directly via RNAPII.

We next determined whether Cdk11 kinase activity is required for centromeric transcription. We transfected HeLa Tet-on cells stably expressing Myc-Cdk11-p110 WT or KD with Cdk11 siRNAs and then extracted total RNAs for real-time PCR analysis. Expression of Myc-Cdk11-p110 WT, not KD, largely restored the decreased α-Sat-4 and α-Sat13/21 RNAs in Cdk11-depleted cells, while it had varying effects on the expression of the tested genes (Figure 7D). Thus, Cdk11 kinase activity is required for efficient centromeric transcription.

Previous studies showed that Cdk11 knockdown can alter cell-cycle profile (Hu *et al*., 2007; Zhou *et al*., 2015), suggestive of a possibility that Cdk11-knockdown–caused change of centromeric transcription could be due to an alteration of cell-cycle profile. To address this concern, we firstly examined how centromeric transcription is regulated during the cell cycle. We arrested HeLa Tet-On cells with thymidine (G1), RO-3306 (G2) and nocodazole (M) and then extracted total RNAs for real-time PCR analysis. We found that G1-arrested cells had a slightly higher level of centromeric transcription than G2-arrested and M-phase cells (Figure 7E). Thus, centromeric transcription is cell cycle regulated, but not very strictly. Our FACS analyses showed a slight change in cell-cycle profile induced by Cdk11 knockdown with decrease in G1 population by ~16% and increase in G2 population by ~10% (Supplemental Figure S5, A and B). Such minor change unlikely accounted for a significant reduction in centromeric transcription in Cdk11-knockdown cells. As centromeric transcription peaks at G1 phase, we then determined whether Cdk11 is required for efficient centromeric transcription in G1 phase. By examining centromeric transcription in thymidine-arrested cells depleted of Cdk11, we found that Cdk11 is required for efficient centromeric transcription in G1 phase (Figure 7F). Taken these results together, Cdk11-knockdown–decreased centromeric transcription is unlikely due to an alteration of cell-cycle profile. We noticed

color-coded. The average and SD calculated from means of three biological replicates are shown here. Differences were assessed using ANOVA followed by pairwise comparisons using Tukey's test. Two-tailed test were used. (C) Targeting Bub1 kinase domain to kinetochores by Mis12 partially rescues centromeric cohesion defects in Cdk11-knockdown cells. HeLa Tet-On cells treated with luciferase (mock) or Cdk11 siRNAs were transfected with vector or GFP-Mis12-Bub1 (631-1085) WT or KD. Cells were then treated with nocodazole for 2 h and mitotic cells were collected for chromosome spread and immunostained with the indicated antibodies. Scale bars, 5 μm and 1 μm, respectively. (D) Quantifications of the distance of inter-sister centromeres and GFP levels on kinetochores (GFP/ACA, bottom panel) in (C). In the top panel, a total of 340, 361, 392, and 390 centromeres were scored for mock, siCdk11 #1, GFP-Mis12-Bub1 WT and KD, respectively; in the bottom panel, 188, 210, 196, and 204 centromeres were scored for mock, siCdk11 #1, GFP-Mis12-Bub1 WT and KD, respectively. The pooled data is grey-coded. The mean calculated from each biological replicate is color-coded. The average and SD calculated from means of three biological replicates are shown here. Differences were assessed using ANOVA followed by pairwise comparisons using Tukey's test. Two-tailed test were used. I Quantification of chromosome morphology with distinct Sgo1 localization patterns (types I, II, and III) in (C), described in (Figure 1F). In total, 91, 84, 103, and 85 cells were scored for mock, siCdk11 #1, GFP-Mis12-Bub1 WT and KD, respectively. The pooled data is grey-coded. The mean calculated from each biological replicate is color-coded. The average and standard error calculated from three independent experiments are shown here. Scale bar, 1 μm. Differences were assessed using ANOVA followed by pairwise comparisons using Tukey's test. Two-tailed test were used. (F) Lysates of HeLa Tet-On cells treated with mock or distinct Cdk11 siRNAs were resolved with SDS–PAGE and blotted with the indicated antibodies. Asterisk indicates nonspecific protein bands. The black line indicates the membrane was cropped. The blots were run under the same experimental conditions and cropped from same membrane. ns denotes not significant; *, $P < 0.05$; **, $P < 0.01$; ***, $P < 0.001$.

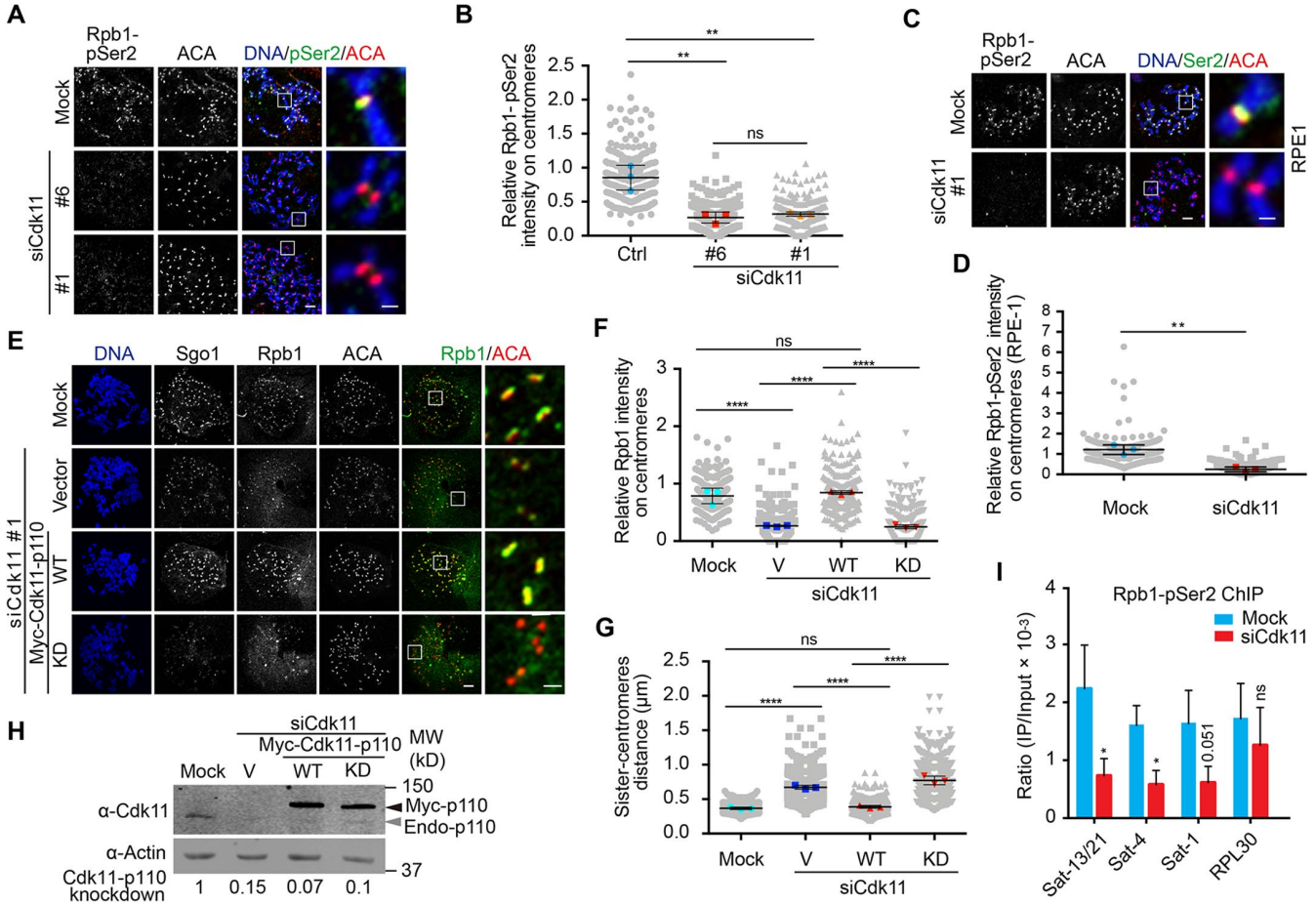

FIGURE 3: RNAPII and RNAPII pSer2 levels on centromeres are reduced by Cdk11 knockdown. (A) Cdk11 decreases RNAPII pSer2 (Rpb1-pSer2) levels on centromeres in HeLa Tet-On cells during mitosis. Nocodazole-arrested HeLa Tet-On cells were transfected with luciferase (mock) or distinct Cdk11 siRNAs. Mitotic cells were subjected to chromosome spread and immunostaining with the indicated antibodies. Antibody H5 was used to recognize RNAPII phosphorylated at Ser2. Scale bars, 5 μm and 1 μm, respectively. B. Quantification of relative Rpb1-pSer2 (Rpb1-pSer2/ACA) in (A). The quantification was performed based on three independent experiments. In total, 246, 252, and 246 centromeres were scored for mock, siCdk11 #6, and siCdk11 #1, respectively. The pooled data is grey-coded. The mean calculated from each biological replicate is color-coded. The average and SD calculated from means of three biological replicates are shown here. Differences were assessed using ANOVA followed by pairwise comparisons using Tukey's test. Two-tailed test were used. (C and D) Cdk11 decreases RNAPII pSer2 (Rpb1-pSer2) levels on centromeres in RPE-1 cells during mitosis. RPE-1 cells treated with the same condition as in (A) were subjected to chromosome spread and immunostaining with the indicated antibodies (C). Scale bars, 5 μm and 1 μm, respectively. Quantification of relative Rbp1-pSer2 is shown in (D). The quantification was performed based on three independent experiments. In total, 258 and 258 centromeres were scored for mock and siCdk11 #1, respectively. The pooled data is grey-coded. The mean calculated from each biological replicate is color-coded. The average and SD calculated from means of three biological replicates are shown here. Differences were assessed using *t* test. Two-tailed test were used. (E) Cdk11 activity maintains RNAPII (Rpb1) on centromeres in HeLa Tet-On cells during mitosis. HeLa Tet-On cells treated with luciferase (mock) or Cdk11 siRNAs were transfected with vector or Myc-Cdk11-p110 WT or KD. Cells were then treated with nocodazole for 2 h and mitotic cells were collected for chromosome spread and immunostaining with the indicated antibodies. Antibody 4H8 was used to recognize total RNAPII. Scale bars, 5 μm and 1 μm, respectively. (F and G) Quantifications of relative Rpb1 levels (Rpb1/ACA, F) and the distance of inter-sister centromeres (G) in (E). These quantifications were performed based on three independent experiments. In (F), 209, 220, 226, and 220 centromeres were scored for mock, siCdk11 #1, Cdk11-p110 WT and KD, respectively; and in (G), 692, 813, 840, and 812 sister-centromere pairs were scored for mock, siCdk11 #1, Cdk11-p110 WT and KD, respectively. The pooled data is grey-coded. The mean calculated from each biological replicate is color-coded. The average and SD calculated from the means of three biological replicates are shown here. Differences were assessed using ANOVA followed by pairwise comparisons using Tukey's test. Two-tailed test were used. (H) Cell lysates from (E) were resolved with SDS–PAGE and blotted with the indicated antibodies. The numbers in the bottom panel indicate Cdk11-p110 knockdown efficiency (Cdk11/Actin). (I) RNAPII pSer2 is associated with centromeric chromatin. Log-phase HeLa Tet-On cells were crosslinked with formaldehyde and the subsequent lysates were subjected to chromatin ChIP assay. Antibody Active Motif was used to recognize RNAPII phosphorylated at Ser2. IP DNA fragments were analyzed with the indicated primers by real-time PCR. The average of ratios (IP/Input × 10^{-3}) and stand deviation calculated from three independent experiments are shown here. Differences were assessed using *t* test. Two-tailed test were used. ns denotes not significant; **, $P < 0.01$; ***, $P < 0.001$.

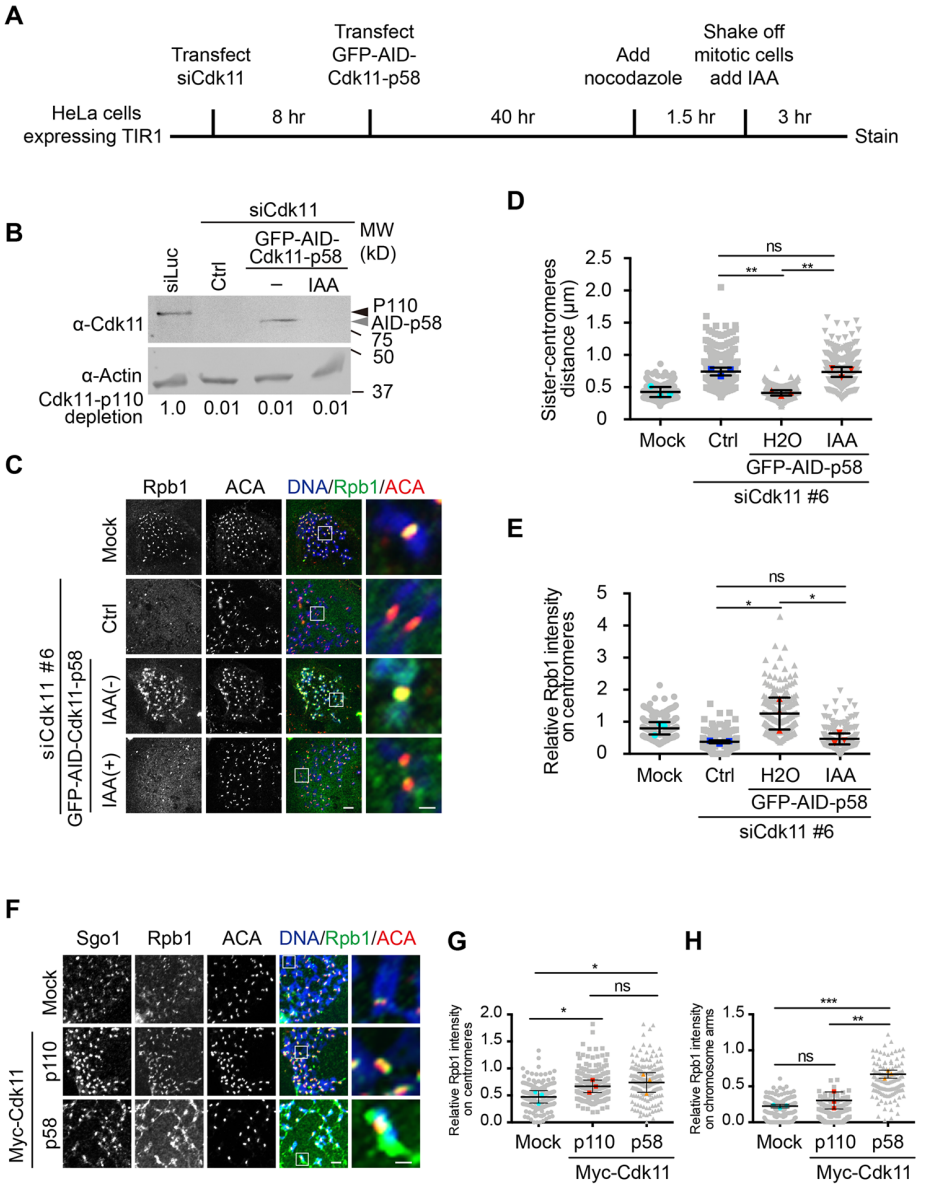

FIGURE 4: Mitosis-specific degradation of Cdk11-p58 or inhibition of Cdk11 reduces RNAPII levels on centromeres and weakens centromeric cohesion. (A) Schematic of Auxin (IAA)-inducible degradation of Cdk11-p58 in mitosis. (B and C) IAA-induced degradation of Cdk11-p58 reduces RNAPII levels on centromeres and weakens centromeric cohesion during mitosis. HeLa Tet-On cells stably expressing Myc-Tir1 were treated with luciferase (mock) or Cdk11 siRNAs and transfected with vectors or plasmids containing GFP-AID-Cdk11-p58. Nocodazole-arrested mitotic cells were collected and further treated with IAA for 3 h. Cells were finally subjected to immunostaining with the indicated antibodies in (C) or analyzed by Western blotting (B). Scale bars, 5 μm and 1 μm, respectively. (D and E) Quantifications of relative Rpb1 levels (Rpb1/ACA, E) and the distance of inter-sister centromeres (D) in (C). These quantifications were performed based on three independent experiments. In (D), 351, 371, 372, and 390 centromeres in total were scored for mock, siCdk11 #6, GFP-AID-Cdk11-p58 IAA(-) and GFP-AID-Cdk11-p58 IAA(+), respectively; in (E), 204, 194, 210, and 228 centromeres in total were scored for mock, siCdk11 #6, GFP-AID-Cdk11-p58 IAA(-) and GFP-AID-Cdk11-p58 IAA(+), respectively. The pooled data is grey-coded. The mean calculated from each biological replicate is color-coded. The mean and SD calculated from means of three biological replicates are shown here. Differences were assessed using ANOVA followed by pairwise comparisons using Tukey's test. Two-tailed test were used. (F) Cdk11-p58 overexpression increases RNAPII levels on both centromeres and chromosome arms. Inducible HeLa cells Tet-On cells with Myc-Cdk11-p110 or Myc-Cdk11-p58 were treated with doxycycline. Cells were treated with nocodazole and then subjected to chromosome spread and immunostaining with the indicated antibodies. Scale bars, 5 μm and 1 μm, respectively. (G and H) Quantifications of relative Rpb1 levels on centromeres (Rpb1/ACA, G) and on chromosome arms (Rpb1/DNA, H). These quantifications were performed based on three independent experiments. In (G), a total of 204, 216, and 215 centromeres for mock, Myc-Cdk11-p110, and Myc-Cdk11-p58 were scored, respectively; in (H), a total of 132 chromosome arms were scored for each condition. The pooled data is grey-coded. The mean calculated from each biological replicate is color-coded. The mean and SD calculated from means of three biological replicates are shown here. Differences were assessed using *t* test (G) and using ANOVA followed by pairwise comparisons using Tukey's test (H). Two-tailed test were used. ns denotes not significant; *, $P < 0.05$; **, $P < 0.01$; ***, $P < 0.001$.

the variation of GAPDH mRNA levels in our experiments, However, even in times when the decrease of GAPDH mRNA levels was statistically significant, it was still marginal (<20%) compared with the decrease of centromere RNA levels. The decrease of centromere RNA levels is pretty robust and dramatic regardless of GAPDH mRNA levels. As Cdk11 also localizes to GAPDH genes (Figure 5F), GAPDH expression might also be subjected to Cdk11 regulation. Variation of GAPDH mRNA levels across our experiments might be due to the variation of Cdk11-knockdown efficiencies.

Overexpression of centromeric α-satellite RNAs rescues Cdk11-knockdown defects

If Cdk11-knockdown–induced centromeric cohesion defects were a consequence of decreased centromeric transcription, ectopic expression of centromeric α-satellite RNAs should be able to rescue the centromeric cohesion defects. We firstly tested whether ectopic expression of centromeric α-satellite RNAs in Cdk11-knockdown cells would restore centromeric transcription. To do so, we cloned alpha-satellite DNA fragments into human expression vector pCS2 using α-satellite primers α-Sat-1, α-Sat-4, and α-Sat-13/21. The molecular sizes of these fragments are ~170 bps. We transfected the mixture-1 or -2 of these plasmids containing these alpha-satellite DNA fragments into HeLa Tet-On cells of Cdk11 knockdown and then examined centromeric cohesion. PCR analyses confirmed that the levels of α-Sat-1, α-Sat-4, and α-Sat-13/21 RNAs were overexpressed in Cdk11-knockdown cells (Figure 8A). We then examined whether ectopic expression of centromeric α-satellite RNAs would restore Cdk11 knockdown defects. Remarkably, overexpression of these centromeric α-satellite RNAs almost completely rescued

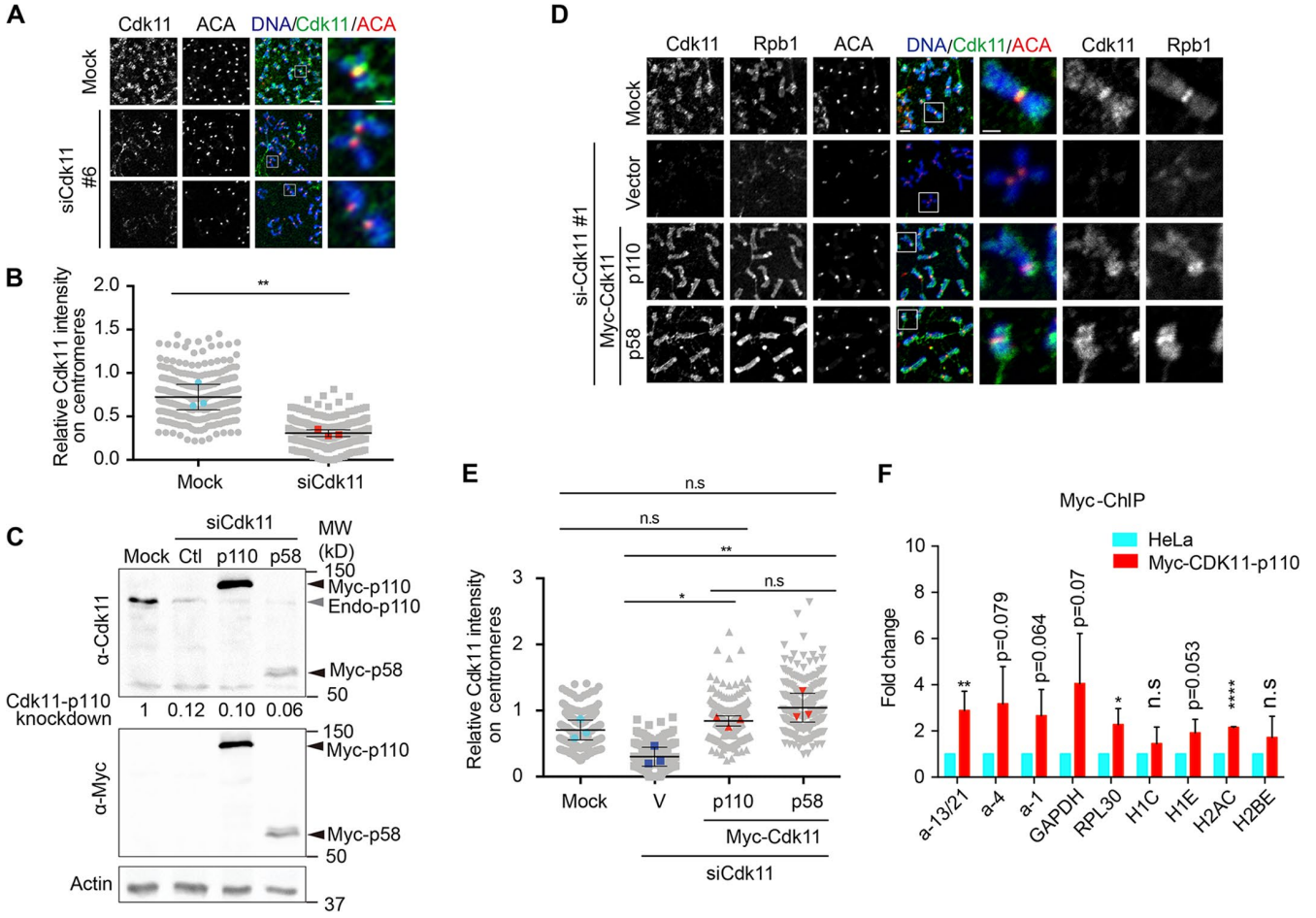

FIGURE 5: Cdk11 associates with centromeres in mitosis and interphase. (A) Cdk11 localizes on mitotic chromosomes and enriches on centromeres. HeLa cells Tet-On cells were treated with nocodazole and then subjected to chromosome spread and immunostaining with the indicated antibodies. Scale bars, 5 μm and 1 μm, respectively. (B) Quantification of relative Cdk11 levels on centromeres (Cdk11/ACA) in (A). These quantifications were performed based on three independent experiments. In total, 216 centromeres were scored for each condition. The pooled data is grey-coded. The mean calculated from each biological replicate is color-coded. The mean and SD calculated from means of three biological replicates are shown here. Differences were assessed using *t* test. Two-tailed test were used. (C) Lysates of log-phase or mitotic HeLa Tet-On cells treated with mock or distinct Cdk11 siRNAs were resolved with SDS–PAGE and blotted with the indicated antibodies. Black arrowhead indicates Cdk11-p110, grey arrowhead indicates Cdk11-p58, and asterisk indicates nonspecific protein bands. The blots were run under the same experimental conditions and cropped from same membrane. (D) Both Cdk11-p110 and -p58 localize on centromeres of mitotic chromosomes. Inducible HeLa Tet-On cells expressing myc-Cdk11-p110 and -p58 were treated with doxycycline and depleted of endogenous Cdk11. Cells were then treated with nocodazole and then subjected to chromosome spread and immunostaining with the indicated antibodies. Scale bars, 5 μm and 1 μm, respectively. (E) Quantification of relative Cdk11 levels on centromeres (Cdk11/ACA) in (A). These quantifications were performed based on three independent experiments. In total, 240, 234, 252, and 264 centromeres were scored for mock, siCdk11 #1, myc-Cdk11 p110 and myc-Cdk11 p58, respectively. The pooled data is grey-coded. The mean calculated from each biological replicate is color-coded. The mean and SD calculated from means of three biological replicates are shown here. Differences were assessed using ANOVA followed by pairwise comparisons using Tukey's test. Two-tailed test were used. (F) Cdk11 is associated with centromeric chromatin in interphase. Log-phase inducible HeLa Tet-On cells with Myc-Cdk11-p110 were treated with doxycycline. Collected cells were crosslinked with formaldehyde and the subsequent lysates were subjected to chromatin ChIP assay. IP DNA fragments were analyzed with the indicated primers by real-time PCR. The mean of normalized fold changes (IP/Input) and stand error calculated from three independent experiments are shown here. Differences were assessed using ANOVA followed by pairwise comparisons using *t* test. Two-tailed test were used. ns denotes not significant; *, $P < 0.05$; **, $P < 0.01$; ****, $P < 0.0001$.

the centromeric cohesion defects caused by Cdk11 knockdown (Figure 8, B and C). At the same time, the levels of Bub1, Knl1-pMELT, Sgo1, and RNAPII on centromeres were also completely restored (Figure 8, D–G). Although these interesting results further confirm the important role of the Cdk11-cenRNA pathway in centromeric cohesion (Figure 8H), they may suggest a more complicated regulatory network for centromeric cohesion and centromeric transcription. On one hand, Cdk11-cenRNA promotes centromeric cohesion; on the other hand, the retained cohesin on centromeres strengthens RNAPII transcription, as suggested by a previous report

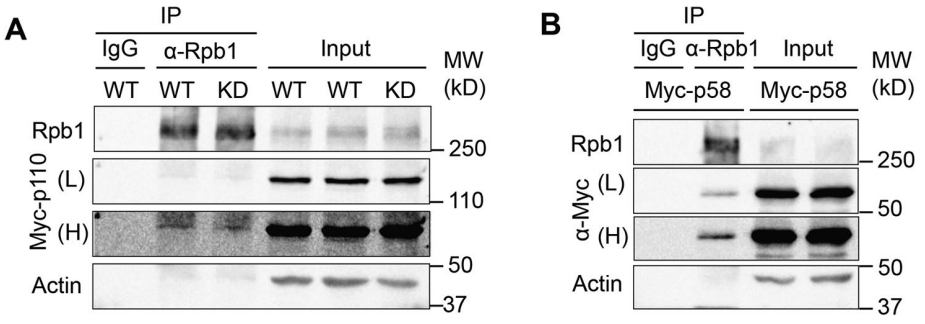

FIGURE 6: Cdk11 binds RNAPII in cells. (A and B) Cdk11-p110 and Cdk11-p58 bind RNAPII in cells. Log-phase inducible HeLa Tet-On cells with Myc-Cdk11-p110 (A) or p58 (B) were treated with doxycycline. The subsequent cell lysates were treated with IgG or antibody against Rpb1. Immunoprecipitated proteins were finally resolved with SDS–PAGE and blotted with indicated antibodies. L indicates light exposure and H indicates high exposure.

(Perea-Resa *et al.*, 2020), and might also alleviate some kinetochore defects.

DISCUSSION

Centromeric transcription is a conserved process across species and plays an essential role in centromere functions, but a little is known about how centromeric transcription is regulated. We here identify Cdk11 as an important regulator for centromeric transcription. Cdk11 localizes to centromeres and interacts with and phosphorylates centromeric RNAPII to facilitate centromeric transcription, thus maintaining centromeric cohesion that is essential for faithful chromosome segregation in mitosis.

Ser2 phosphorylation of the RNAPII CTD is essential for RNAPII elongation during transcription. Cdk9 is the major kinase that phosphorylates that site, thus rendering Cdk9 a general transcriptional factor (Chou *et al.*, 2020). As a relative to Cdk9, Cdk11 has also been shown to regulate transcription. However, distinct from Cdk9, Cdk11 appears not to universally regulate transcription; instead, it may do so only for a subset of genes (Drogat *et al.*, 2012; Gajduskova *et al.*, 2020). Consistent with this idea, our findings here suggest that Cdk11 is also required for the efficient transcription on a specialized chromosomal region, the centromere, thus establishing a novel role of Cdk11 in transcriptional regulation of noncoding DNA sequences. Mechanistically, Cdk11 localizes on centromeric chromatin where it binds and phosphorylates the RNAPII CTD to maintain elongating RNAPII on centromeres. However, it is worth mentioning that Cdk11-regulated transcription is not specific to centromeres, and it is also important for a subset of genes as demonstrated by Cdk11 association with gene regions besides centromeres. In support of it, we found that Cdk11 localizes to gene regions and mitotic chromosomes (Figure 5F). Recently, we showed that Cdk9 is also critical for centromeric transcription (Chen *et al.*, 2021). Thus, Cdk11 and Cdk9 may play a redundant role in promoting RNAPII elongation on centromeres. In support of this idea, Cdk11 knockdown only resulted in a moderate reduction in centromeric transcription (Figure 7).

When cells enter mitosis, the majority of RNAPII and transcriptional factors are released from chromosomes, leading to a significant loss of RNAPII transcription on chromosomes (Parsons and Spencer, 1997; Palozola *et al.*, 2017; Teves *et al.*, 2018). However, robust levels of elongating RNAPII are remained on centromeres and centromeres are under active transcription during mitosis (Chan *et al.*, 2012; Liu *et al.*, 2015; Bobkov *et al.*, 2018; Perea-Resa *et al.*, 2020; Chen *et al.*, 2021). Thus, a mitosis-specific mechanism may exist to preserve RNAPII on centromeres, thus maintaining a considerable transcriptional activity. Cdk11 may be part of such a mechanism. In support of it, a significant pool of Cdk11 remains at the centromeres of mitotic chromosomes despite removal of most transcription factors (Figure 5, A and B), mitosis-specific degradation of G2/M Cdk11-p58 largely decreased the RNAPII levels on centromeres, and overexpression of Cdk11-p58 increased RNAPII levels on both centromeres and chromosome arms during mitosis (Figure, 4, F–H). Of note, because we showed in this study that expression of either Cdk11-p110 or -p58 completely restored centromeric Cdk11 and Rbp1 levels and cohesion defects (Figure 3F, 5D; Supplemental Figures S3 and S4D), it is likely that both Cdk11-p110 and -p58 are needed to maintain centromeric transcription during mitosis. The isoform of p58 that is exclusively expressed in G2/mitosis may provide an extra insurance for the maintenance of centromeric transcription during mitosis.

How is Cdk11 involved in centromeric cohesion regulation? This question had not been adequately addressed because the first discovery of Cdk11 involvement in the regulation of centromeric cohesion a decade ago. Although previous studies had thrown Bub1 under a spotlight (Hu *et al.*, 2007; Rakkaa *et al.*, 2014), our data here suggest that other factors beyond Bub1 are also involved in Cdk11-regulated cohesion. Specifically, ectopic restoration of fully functional Bub1 on kinetochores only partially rescued centromeric cohesion defects in Cdk11-knockdown cells. Here, we have established Cdk11 as an important regulator for centromeric transcription and this role may empower Cdk11 to regulate centromeric cohesion (Figure 8H). This conclusion is further supported by our genetic data showing that the overexpression of centromeric α-satellite RNAs fully rescued the weakened centromeric cohesion induced by Cdk11 knockdown (Figure 8, A–C). Further experimentation revealed that the overexpression of centromeric α-satellite RNAs also restored the levels of Knl1-pMELT, Bub1, Sgo1, and RNAPII on centromeres (Figure 8, E–G), suggesting a more complicated regulatory network for centromeric cohesion and centromeric transcription. On one hand, Cdk11-cenRNA promotes centromeric cohesion; on the other hand, the retained cohesin on centromeres would strengthen RNAPII transcription.

Notably, previous studies showed that defective mRNA splicing induced centromeric cohesion defects through decreasing the protein levels of an essential cohesion protector Sororin (Oka *et al.*, 2014; Sundaramoorthy *et al.*, 2014; van der Lelij *et al.*, 2014; Watrin *et al.*, 2014). Considering a role of Cdk11 in mRNA splicing (Loyer *et al.*, 1998; Dickinson *et al.*, 2002; Trembley *et al.*, 2002; Hu *et al.*, 2003; Loyer *et al.*, 2008; Valente *et al.*, 2009; Pak *et al.*, 2015), centromeric cohesion defects caused by Cdk11 could also be attributed to compromised mRNA splicing. Although our results here have largely excluded the involvement of Sororin and several other cohesion-regulators, we cannot completely rule out the possibility that Cdk11 promotes centromeric cohesion through regulating mRNA splicing for some other yet-to-be-identified cohesion regulators. Nevertheless, our findings in this report provide a novel mechanism that further elucidates the importance of Cdk11 in centromeric cohesion and further highlight the emerging critical role of centromeric transcription in centromeric cohesion regulation (Liu *et al.*, 2015; Liu, 2016; Chen *et al.*, 2021). Notably, The centromeric transcription-cohesion relationship may also explain why a

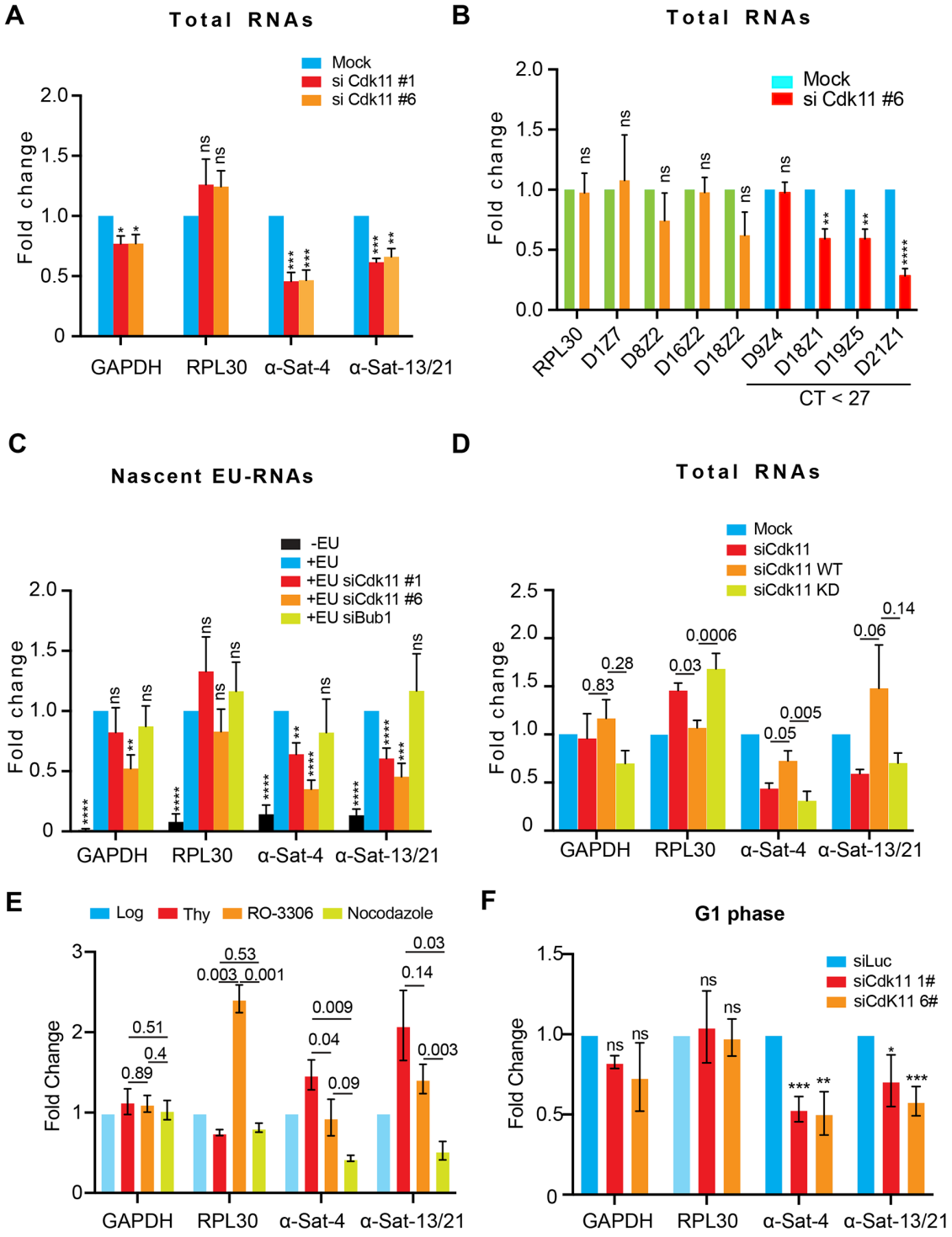

FIGURE 7: Cdk11 knockdown decreases centromeric alpha-satellite RNAs. (A) Cdk11 knockdown reduces the amount of centromeric alpha-satellite RNAs. Total RNAs were extracted from HeLa Tet-On cells transfected with mock or distinct Cdk11 siRNAs. Real-time PCR was performed to evaluate the amount of RNAs as indicated. The mean and stand error calculated from four independent experiments are shown here. Differences were assessed using ANOVA followed by pairwise comparisons using Tukey's test. Two-tailed test were used. (B) Cdk11 knockdown reduces the amount of centromeric satellite RNAs derived from HOR primers. Total RNAs were extracted from HeLa Tet-On cells transfected with mock or Cdk11 siRNAs. Real-time PCR was performed to evaluate the amount of RNAs as indicated. The average and stand error calculated from three independent experiments are shown here. Differences were assessed using *t* test. Two-tailed test were used. (C) Cdk11 knockdown decreases the amount of centromeric alpha-satellite nascent EU-RNAs. Log HeLa Tet-On cells transfected with luciferase (mock) or distinct Cdk11 siRNAs were treated with EU 1 h before harvest. EU-RNAs were purified and then subjected to real-time analysis with the indicated primers. The mean and stand error calculated from at least four independent experiments are shown here. Differences were assessed using *t* test. Two-tailed test were used. (D) Cdk11 kinase activity is required for maintaining the amount of centromeric

transcriptional regulator prohibitin 2 (PHB2) is important for centromeric cohesion regulation (Takata *et al*., 2007). In further, it would be of importance to identify more key factors that are specific and important for centromeric transcription as well as to explore the molecular mechanism through which centromeric transcription promotes centromeric cohesion.

MATERIALS AND METHODS

Mammalian cell culture, siRNAs, and transfection

Hela Tet-on cells were cultured in DMEM, Invitrogen containing 10% fetal bovine serum (FBS) and 10 mM L-glutamine at 37°C and 5% CO_2. RPE-1 cells were cultured in DMEM: F-12 medium (Invitrogen) supplemented with 10% FBS and 10 mM L-glutamine. To arrest cells at G1/S, cells were usually incubated in medium containing 2 mM thymidine (Sigma) for at least 16 h. To arrest cells at G2, thymidine-arrested cells were released and inbubated in medium containing 1 μM RO3306 for 16 h. To arrest cells at mitosis, thymidine-arrested cells were released and incubated in medium containing 500 nM nocodazole for 12 h. RO3306 and nocodazole were purchased from Sigma Aldrich.

Plasmid transfection was implemented using the Effectene reagent (Qiagen) according to the manufactures' protocols. For Myc-Cdk11 (WT or KD) or Myc-Cdk11-p58 WT stable cells, Hela Tet-on cells were transfected with pTRE2 vectors encoding RNAi-resistant Myc-Cdk11 or Myc-Cdk11-p58 and selected with 350 μg ml^{-1} hygromycin (Invitrogen). The surviving clones were screened for expression of the desired proteins in the presence of 1 μg ml^{-1} doxycycline (Invitrogen). Expression of Myc-Cdk11 was also induced with 1 μg ml^{-1} doxycycline in the subsequent experiments.

For RNAi experiments, siRNA oligonucleotides were purchased from Dharmacon. HeLa or RPE-1 cells were transfected using Lipofectamine RNAiMax (Invitrogen) according to the manufacturer's protocols. Subsequent analyses were usually performed 48 h after transfection with siRNAs unless specified. The sequences of the siRNAs used in this study are: siBub1, CCCAUUUGCCAGCUCAAGCTT; siCdk11 #1, AGCGGCUGAAGAUGGAGAA; siCdk11 #6, GAGCGAGCAGCAGCGUGUGUU; siCdk11 #2, GAUGAAAUUGUGGCUCUAA (MU-004687-02, Dharmacon); siCdk11 #3, UGAAACACCUGCACGACAA (MU-004687-03, Dharmacon); siCdk11 #4, UAAAGCGGCUGAAGAUGGA (MU-004687-04, Dharmacon); siCdk11 #5, CAGAUGAAAUUGUGGCUCU (MU-004687-05, Dharmacon).

Antibodies, immunoblotting, and IP

Antibodies used in this study were listed in the following: anti-centromere antibody (ACA or CREST-ImmunoVision, HCT-0100), anti-Actin (Invitrogen, MA5-11869), anti-GFP (Abcam, ab1218), anti-Myc (Roche, 11667203001), anti-Smc1 (Bethy, A300-055A), anti-Rpb1 (Abcam, 4H8, ab5408), anti-Rpb1-pSer2 (Biolegend, H5; ActiveMotif, 61083), anti-Cdk11 (Bethy, A300-310A; Abcam, ab19393). Anti-APC2, anti-Sgo1, and anti-Bub1 antibodies were made in-house as described previously (Liu *et al*., 2015). Anti-Sororin antibody was a gift from Dr. Susannah Rankin.

For immunoblotting, the secondary antibodies were purchased from Li-COR: IRDye 680RD Goat anti-Mouse IgG Secondary Antibody (926-68070) and Goat anti-Rabbit IgG Secondary Antibody (926-32211).

IP was performed as follows. Cells were cross-linked with buffer (50 mM HEPES, pH 8.0, 1% formaldehyde, 100 mM NaCl, 1 mM ethylenediaminetetraacetic acid [EDTA], and 0.5 mM ethylene glycol-bis(β-aminoethyl ether)-*N*,*N*,*N*′,*N*′-tetraacetic acid [EGTA]) at room temperature for 10 min and further treated with 125 mM Glycine for another 5 min. Cells were resuspended in lysis buffer (25 mM Tris-HCl at pH 7.5, 50 mM NaCl, 5 mM $MgCl_2$, 0.1% NP-40, 1 mM DTT, 0.5 μM okadaic acid, 5 mM NaF, 0.3 mM Na_3VO_4 and 100 units ml^{-1} Turbo-nuclease [Accelagen]). After a 1-h incubation on ice and then a 10-min incubation at 37°C, the lysate was cleared by centrifugation for 15 min at 4°C at 20,817g. The supernatant was incubated with the antibody beads overnight at 4°C. The beads were washed four times with wash buffer (25 mM Tris-HCl at pH 7.5, 50 mM NaCl, 5 mM $MgCl_2$, 0.1% NP-40, 1 mM DTT, 0.5 μM okadaic acid, 5 mM NaF, and 0.3 mM Na_3VO_4). The proteins bound to the beads were dissolved in SDS sample buffer, separated by SDS–PAGE and blotted with the appropriate antibodies.

For immunoblotting, primary and secondary antibodies were used at 1 μg ml^{-1} concentration.

Immunofluorescence and chromosome spread

Chromosome spread was performed as previously described (Yang *et al*., 2021). Cells were treated with 5μM nocodazole for 2 h and mitotic cells were collected after mitotic shake-off. Then mitotic cells were swelled in a prewarmed hypotonic solution containing 75 mM potassium chloride (KCl) for 15 min at 37 °C and then spun onto slides with a Shandon Cytospin centrifuge. Cells were then treated the same as described in the regular staining. Cells were immediately fixed with 4% ice-cold paraformaldehyde for 4 min, and then extracted with ice-cold phosphate-buffered saline (PBS) containing 0.2% Triton X-100 for 2 min. Cells were next washed with PBS containing 0.1% Triton X-100 and then incubated with primary antibodies (1:1000 dilution) overnight at 4°C. After washed with PBS containing 0.1% Triton X-100, cells were incubated at room temperature for 1 h with the appropriate secondary antibodies conjugated to fluophores (Molecular Probes, 1:1000 dilution). After incubation, cells were washed again with PBS

alpha-satellite RNAs. Log-phase inducible HeLa Tet-On cells with Myc-Cdk11-p110 WT (4 or 6) or KD (18 or 22) were treated with doxycycline and transfected with luciferase (mock) or Cdk11 siRNAs. Total RNAs were extracted from HeLa Tet-On cells transfected with mock or distinct Cdk11 siRNAs. Real-time PCR was performed to evaluate the amount of RNAs as indicated. The average and stand error calculated from at least three independent experiments are shown here. Differences were assessed using ANOVA followed by pairwise comparisons using Tukey's test. Two-tailed test were used. (E) Temporal change of centromeric transcription throughout the cell cycle. Total RNAs were extracted from asynchronized HeLa Tet-On cells or cells arrested at G1/S (thymidine), G2 (RO-3306), and mitosis (nocodazole). Real-time PCR was performed to evaluate the amount of RNAs as indicated. The mean and stand error calculated from three independent experiments are shown here. Differences were assessed using ANOVA followed by pairwise comparisons using Tukey's test. Two-tailed test were used. (F) Cdk11 knockdown decreases centromeric transcription in G1 phase. Total RNAs were extracted from thymidine-arrested HeLa Tet-On cells depleted of Cdk11. Real-time PCR was performed to evaluate the amount of RNAs as indicated. The mean and stand error calculated from three independent experiments are shown here. Differences were assessed using *t* test. Two-tailed test were used. ns denotes not significant; *, $P < 0.05$; **, $P < 0.01$; ***, $P < 0.001$; ****, $P < 0.0001$.

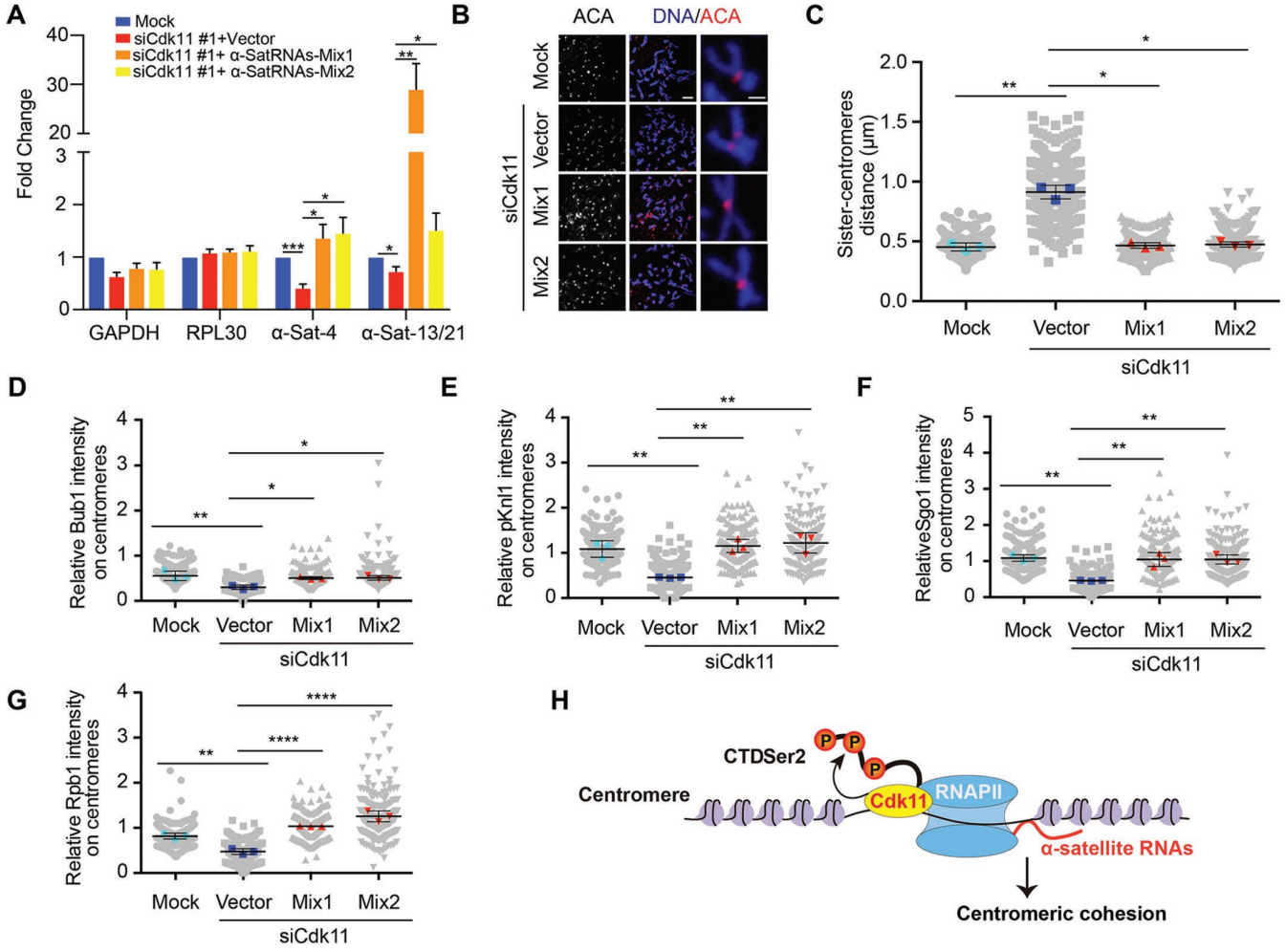

FIGURE 8: Ectopic expression of alpha-satellite RNAs fully rescues Cdk11-knockdown phenotypes. (A) Ectopic expression of alpha-satellite RNAs rescues the reduced levels of cenRNAs in Cdk11-knockdown cells. Log-phase HeLa Tet-On cells treated with luciferase (mock) or Cdk11 siRNAs (#1) were transfected with plasmids containing centromeric alpha-satellite DNA fragments (Mix1 or Mix2). Total RNAs were extracted from cells depleted of Cdk11 for real-time PCR analysis with the indicated primers. The mean and stand error calculated from eight independent experiments are shown here. Differences were assessed using ANOVA followed by pairwise comparisons using Tukey's test. Two-tailed test were used. (B) Ectopic expression of alpha-satellite RNAs rescues centromeric cohesion defects RNAs in Cdk11 depletion. Mitotic cells treated in (A) were collected for chromosome spread and immunostaining with the indicated antibodies. Representatives of microscopic images are shown here. Scale bars, 5 μm and 1 μm, respectively. (C) Quantification of the distance of inter-sister centromeres (B). These quantifications were performed based on three independent experiments. In total, 361, 400, 380, and 380 centromeres were scored for mock, siCdk11 #6, mixture 1 and mixture 2, respectively. The pooled data is grey-coded. The mean calculated from each biological replicate is color-coded. The mean and SD calculated from means of three biological replicates are shown here. Differences were assessed using ANOVA followed by pairwise comparisons using Tukey's test. Two-tailed test were used. (D and E) Quantification of relative Bub1 levels (Bub1/ACA) and Knl1 p-MELT levels (p-MELT/ACA) on centromeres. These quantifications were performed based on three independent experiments. In total, 204, 198, 198, and 203 centromeres were scored for mock, siCdk11 #1, mixture 1 and mixture 2, respectively. The pooled data is grey-coded. The mean calculated from each biological replicate is color-coded. The mean and SD calculated from means of three biological replicates are shown here. Differences were assessed using ANOVA followed by pairwise comparisons using Tukey's test. Two-tailed test were used. (F and G) Quantification of relative Sgo1 levels (Sgo1/ACA) and Rpb1 levels (Rpb1/ACA) on centromeres. These quantifications were performed based on three independent experiments. In total, 216, 222, 222, and 216 centromeres were scored for mock, siCdk11 #1, mixture 1 and mixture 2, respectively. The pooled data is grey-coded. The mean calculated from each biological replicate is color-coded. The mean and SD calculated from means of three biological replicates are shown here. Differences were assessed using ANOVA followed by pairwise comparisons using Tukey's test. Two-tailed test were used. (H) Working model. Constitutively expressed Cdk11 binds RNAPII and phosphorylates CTD-Ser2 at centromeres to promote centromeric transcription in both interphase and mitosis. G2/M-expressed Cdk11-p58 may facilitate the retention of RNAPII on centromeres during mitosis, thus helping maintain centromeric transcription and centromeric cohesion. *, $P < 0.05$; **, $P < 0.01$; ****, $P < 0.0001$.

containing 0.1% Triton X-100, stained with 1 μg ml^{-1} DAPI and mounted with Vectashield.

The images were taken by a Nikon inverted confocal microscope (Eclipse Ti2, NIS-Elements software) with a × 60 objective. ImageJ and Adobe Photoshop Image processing were used to further process the obtained microscope images. Quantification was performed with ImageJ. Statistical analysis was carried out with GraphPad Prism.

EU chasing and purification of EU-RNAs

Extraction of EU-RNAs was performed according to the protocol from Click-iT Nascent RNA Cpature Kit (C10365, Thermo Fisher Scientific). EU in a final concentration of 0.5 mM was added into for cells with a confluency of 60-80% in 10 cm petri dishes 1 h before harvest. Then collected EU-chased cells were dissolved in TRIzol solution (Invitrogen, 15596026) and extracted total RNAs were dissolved in nuclease-free water. After being further treated with TURBO DNase (Invitrogen, AM2238) in the presence of RNase inhibitor (NEB, M3014) at 37°C for 1 h, total RNAs were then extracted with Phenol/Chloroform/Isoamyl alcohol (Invitrogen, 15593-031), precipitated with ice-cold ethanol solution containing glycogen (Roche, 34990920) and sodium acetate (Invitrogen, AM9740), and finally dissolved in nuclease-free water (Invitrogen, 10977-015). Purified total RNAs were then further incubated with streptavidin dynabeads (Invitrogen, 65602) pretreated with Salmon sperm DNA (Invitrogen, 15632011) in binding buffer for 45 min. With the help of DynaMag^{TM}-2 Magnet (Invitrogen 12321D), dynabeads were washed with wash buffer I and II. Washed dynabeads were ready for later analyses.

Reverse transcription and real-time PCR analysis

EU-RNA bound dynabeads were mixed with iScript Reverse Transcription Supermix (Bio-Rad, 1708841) and reverse transcription was carried out according to the manufacturer's protocols Synthesized cDNAs were mixed with the SsoAdbanced Universal SYBR Green Supermix (Bio-Rad, 1725274) and then subjected to real-time PCR analysis using QuantStudio 6 Flex Real-Time PCR System (Applied Biosystems).

The primers for human cells were used in this study: GAPDH-F: 5′-TGATGACATCAAGAAGGTGGTGAAG-3′, GAPDH-R: 5′-TCCTTGGAGGCCATGTGGGCCAT-3′; Rpl30-F: 5′-CAAGGCAAAGCGAAATTGGT-3′, Rpl30-R: 5′-GCCCGTTCAGTCTCTTCGATT-3′; SAT-4-F: 5′-CATTCTCAGAAACTTCTTTGTGATGTG-3′, SAT-4-R: 5′-CTTCTGTCTAGTTTTTATGTGAATATA-3′; SAT-13/21-F: 5′-TAGACAGAAGCATTCTCAGAAACT-3′; SAT-13/21-R: 5′-TCCCGCTTCCAACGAAATCCTCCAAAC-3′. Intergenetic-1: CCAAACTTGCTTACTCCAAAGC; ATTCCAACCCAGAACCCAGA. Intergenetic-2: GGCAAATAGTCAACTTTCACTGC; CTATGGGAGGGTTGCTTTGA. Both the Intergenetic primers were described in (Khaitovich *et al*., 2006).

Ectopic expression of alpha-satellite RNAs

Alpha-satellite DNA fragments were cloned into PC2 vectors with RNAPII promotes. The generated plasmids were transfected into HeLa cells for 48 hrs. Cells were then collected for further analysis. The sequences of alpha-satellite DNA fragments mix1 (1, 4, and 13-1) and mix2 (1, 4, and 13-2) are as follows:

1. CAACGAAGGCCACAAGATGTCAGAATATCCACTTACAGACTTTACAAACAGAGTGTTTCCTAACTGGTCTATGAACAGAAAGTTTAAACTCTGTGAGTTGAACGAACACATCACAACGCAGTTTGTGGGAATGATTCTGTCTAGTTTTGAAACGAAGATATTTCCTTTTCTGCCATTGACCTT

4. CTTCTGTCTAGTTTTTATGTGAAGATATTTCCTTCTTCACCACAGGCCTCAAAGTGCTCCAAATATTCATTTGCAGATTCTACAAAGAGACTCTTTCCAAACTGCTCAATCAAAAGAAAGATTGATCTCTTTGAGATGAAAGCACACATCACAAAGAAGTTTCTGAGAATG

13-1. TAGACAGAAGCATTCTCAGAAACTTGTTGGTGATATGTGTCCTCAACTAACAGAGTTGAACTTTGCCATTGATAGAGAGCAGTTTTGAAACACTCTTTTTGTGGAATCTGCAAGTGGATATTTGGATAGCTTGGAGGATTTCGTTGGAAGCGGGA

13-2. TCCCGCTTCCAACGAAATCCTCCAAGCTATCCAAATATCCACTTGCAGATTCCACAGAAAGACTGTTTCAAAACTGCTCTGTCAATAGAAAGGTTCAACTCTGTTAGCTGCGTGCATATATCCCAAAGAAGATTCTGAGATTGCTTCTGTCTAGTTTTTATGGGAAGATATTTCCCTTTTCACCGTAGGCGTCAAGGCGCTCCAAATGTCCACTTCCAGATACTACAAAAAGAGTGTTTCAAACCTACTCTGTGAAAGGGAATATTCAACTCTGTGACTTGAATGCACATATCACAAGGAAGTTTCTGAGAATGCTTCTGTCTA

Chromatin immunoprecipitation

Cells were firstly cross-linked by formaldehyde with buffer (50 mM HEPES, pH 8.0, 1% formaldehyde, 100 mM NaCl, 1 mM EDTA, and 0.5 mM EGTA) at room temperature for 10 min and further treated with 125 mM glycine for another 5 min. After being resuspended in IP buffer (10 mM Tris 8.0, 300 mM NaCl, 1 mM EDTA, 1 mM EGTA, 1% Triton X-100, and 1% sodium deoxycholate), cells were sonicated using a Thermo Fisher Scientific sonicator. Cell debris was removed centrifugation and the supernatant was precleared with protein-A beads (Santa Cruz; SC-2001) at 4°C for 2 h. Precleared cell lysates were then incubated with 5 μg anti-Myc or RNAPII-pSer2 antibodies overnight and further with protein-A beads for another 2 h at 4°C. Pelleted beads were sequentially washed by low salt buffer (20 mM Tris 8.0, 150 mM NaCl, 0.1% sodium dodecyl sulfate (SDS), 1% Triton X-100, and 2 mM EDTA), high-salt buffer (20 mM Tris 8.0, 500 mM NaCl, 0.1% SDS, 1% Triton X-100, and 2 mM EDTA), LiCl buffer (10 mM Tris 8.0, 0.25 M LiCl, 1% octylphenoxypolyethoxyethanol CA630, 1% sodium deoxycholate, and 1 mM EDTA), and TE buffer (10 mM Tris, pH 8.0, and 1 mM EDTA, pH 8.0). Afterward, beads were treated with elution buffer (10 mM Tris 8.0, 1 mM EDTA, and 1% SDS) at 65°C for 10 min, and the elute was further incubated at 65°C overnight to reverse the cross-linking. Then the solution was sequentially treated with RNase A (Qiagen; 1007885) at 37°C for 1 h and Proteinase K (Thermo Fisher Scientific; EO0491) at 50°C for 2 h. Finally, DNA in the solution was extracted with Phenol/Chloroform/Isoamyl alcohol (25:24:1, vol/vol; Invitrogen; 15593-031) and purified by Qiagen gel purification kit for later analyses.

Flow cytometry

Cultured cells were harvested cells by trypsinization, washed with PBS, and fixed with ice-cold 70% ethanol overnight at –20°C. After being washed once with PBS, cells were then permeabilized with PBS containing 0.25% Triton X-100 for 5 min and further stained with propidium iodide (Sigma-Aldrich) at a final concentration of 20 μg/ml. RNase A (QIAGEN) was added at a final concentration of 200 μg/ml. The samples were finally analyzed with BD LSR Fortessa flow cytometer.

Quantification and statistical analysis

Microscope images were imported into Image J. In the quantifications of Figures 1, B and E, 2, B and D, 3, B, D, and F, 4, E and G,

5, B and E, 8, D–G; Supplemental Figures S1C, S2B, S3C and S4D, five or six kinetochores were randomly selected from each cell. A mask was generated to mark centromeres based on ACA fluorescence signals in the projected image. Numeric intensities of these marked signals were obtained. After background subtraction, the intensities of Bub1, Sgo1, Rpb1, Rpb1-Ser2, p-MELT, Cdk11, and ACA signals within the mask were obtained in number. Relative intensity was calculated from the intensity of Bub1, Sgo1, Rpb1, Rpb1-Ser2, or p-MELT signals normalized to the one of ACA signals and plotted with the GraphPad Prizm software.

For quantification of Rpb1 levels on chromosome arms in Figure 4H, a mask was generated to mark a chromosome arm. Numeric intensities of these marked signals were obtained. After background subtraction, the intensities of Rpb1 and DAPI fluorescence signals within the mask were obtained in number. Relative intensity was derived from the intensity of Rpb1 normalized to the one of DAPI signals and plotted with the GraphPad Prism software.

Measurement of sister-centromere distance in Figures 1C, 2D, 3G, 4D, 8C; Supplemental Figures S2A and S3B was carried out with ImageJ. A straight line was drawn between a pair of sister centromeres, revealed by ACA signals. Numeric values were automatically generated by ImageJ.

Quantification was performed based on the results from three independent experiments, which is specified in the legends of each figure. The values were separately pooled for each biological replicate and the mean was calculated for each pool. Those means were then used to calculate the average, SD or standard error, and *P* value. Differences were assessed using ANOVA followed by pairwise comparisons using Tukey's test or *t* test. Two-tailed test were used. All the samples analyzed were included in quantification. Sample size was recorded in figures and their corresponding legends. No specific statistical methods were used to estimate sample size. No methods were used to determine whether the data met assumptions of the statistical approach.

ACKNOWLEDGMENTS

This work was supported by Tulane University startup funds and the National Institute of General Medical Sciences/the National Institutes of Health grants R01GM124018 and R01GM141123, awarded to H.L.. Research reported in this study was also supported by the National Cancer Institute of the National Institutes of Health under Award Number R01CA261258 to Z.L.. The content is solely the responsibility of the authors and does not necessarily represent the official views of the National Institutes of Health.

REFERENCES

Bobkov GOM, Gilbert N, Heun P (2018). Centromere transcription allows CENP-A to transit from chromatin association to stable incorporation. J Cell Biol 217, 1957–1972.

Bury L, Moodie B, Ly J, McKay LS, Miga KH, Cheeseman IM (2020). Alpha-satellite RNA transcripts are repressed by centromere-nucleolus associations. eLife 9, e59770.

Chan FL, Marshall OJ, Saffery R, Kim BW, Earle E, Choo KH, Wong LH (2012). Active transcription and essential role of RNA polymerase II at the centromere during mitosis. Proc Natl Acad Sci USA 109, 1979–1984.

Chen Y, Zhang Q, Teng Z, Liu H (2021). Centromeric transcription maintains centromeric cohesion in human cells. J Cell Biol 220, e202008146.

Chou J, Quigley DA, Robinson TM, Feng FY, Ashworth A (2020). Transcription-associated cyclin-dependent kinases as targets and biomarkers for cancer therapy. Cancer Discov 10, 351–370.

Cornelis S, Bruynooghe Y, Denecker G, Van Huffel S, Tinton S, Beyaert R (2000). Identification and characterization of a novel cell cycle-regulated internal ribosome entry site. Mol Cell 5, 597–605.

Dickinson LA, Edgar AJ, Ehley J, Gottesfeld JM (2002). Cyclin L is an RS domain protein involved in pre-mRNA splicing. J Biol Chem 277, 25465–25473.

Drogat J, Migeot V, Mommaerts E, Mullier C, Dieu M, van Bakel H, Hermand D. (2012). Cdk11-cyclinL controls the assembly of the RNA polymerase II mediator complex. Cell Rep 2, 1068–1076.

Fu TJ, Peng J, Lee G, Price DH, Flores O (1999). Cyclin K functions as a CDK9 regulatory subunit and participates in RNA polymerase II transcription. J Biol Chem 274, 34527–34530.

Gajduskova P, Ruiz de Los Mozos I, Rajecky M, Hluchy M, Ule J, Blazek D. (2020). CDK11 is required for transcription of replication-dependent histone genes. Nat Struct Mol Biol 27, 500–510.

Hluchy M, Gajduskova P, Ruiz de Los Mozos I, Rajecky M, Kluge M, Berger BT, Slaba Z, Potesil D, Weiss E, Ule J, *et al*. (2022). CDK11 regulates pre-mRNA splicing by phosphorylation of SF3B1. Nature 609, 829–834.

Hu D, Mayeda A, Trembley JH, Lahti JM, Kidd VJ (2003). CDK11 complexes promote pre-mRNA splicing. J Biol Chem 278, 8623–8629.

Hu D, Valentine M, Kidd VJ, Lahti JM (2007). CDK11(p58) is required for the maintenance of sister chromatid cohesion. J Cell Sci 120, 2424–2434.

Ishikura S, Nakabayashi K, Nagai M, Tsunoda T, Shirasawa S (2020). ZFAT binds to centromeres to control noncoding RNA transcription through the KAT2B-H4K8ac-BRD4 axis. Nucleic Acids Res 48, 10848–10866.

Jansen LE, Black BE, Foltz DR, Cleveland DW. (2007). Propagation of centromeric chromatin requires exit from mitosis. J Cell Biol 176, 795–805.

Kawashima SA, Yamagishi Y, Honda T, Ishiguro K, Watanabe Y (2010). Phosphorylation of H2A by Bub1 prevents chromosomal instability through localizing shugoshin. Science 327, 172–177.

Khaitovich P, Kelso J, Franz H, Visagie J, Giger T, Joerchel S, Petzold E, Green RE, Lachmann M, Paabo S (2006). Functionality of intergenic transcription: an evolutionary comparison. PLoS Genet 2, e171.

Kitajima TS, Hauf S, Ohsugi M, Yamamoto T, Watanabe Y (2005). Human Bub1 defines the persistent cohesion site along the mitotic chromosome by affecting shugoshin localization. Curr Biol 15, 353–359.

Li T, Inoue A, Lahti JM, Kidd VJ (2004). Failure to proliferate and mitotic arrest of CDK11(p110/p58)-null mutant mice at the blastocyst stage of embryonic cell development. Mol Cell Biol 24, 3188–3197.

Ling YH, Yuen KWY (2019). Point centromere activity requires an optimal level of centromeric noncoding RNA. Proc Natl Acad Sci USA 116, 6270–6279.

Liu H (2016). Insights into centromeric transcription in mitosis. Transcription 7, 21–25.

Liu H, Jia LY, Yu HT. (2013). Phospho-H2A and Cohesin specify distinct tension-regulated Sgo1 pools at kinetochores and inner centromeres. Curr Biol 23, 1927–1933.

Liu H, Qu Q, Warrington R, Rice A, Cheng N, Yu H. (2015). Mitotic transcription installs Sgo1 at centromeres to coordinate chromosome segregation. Mol Cell 59, 426–436.

Loyer P, Trembley JH (2020). Roles of CDK/Cyclin complexes in transcription and pre-mRNA splicing: Cyclins L and CDK11 at the cross-roads of cell cycle and regulation of gene expression. Semin Cell Dev Biol 107, 36–45.

Loyer P, Trembley JH, Lahti JM, Kidd VJ (1998). The RNP protein, RNPS1, associates with specific isoforms of the p34cdc2-related PITSLRE protein kinase in vivo. J Cell Sci 111, 1495–1506.

Loyer P, Trembley JH, Grenet JA, Busson A, Corlu A, Zhao W, Kocak M, Kidd VJ, Lahti JM (2008). Characterization of cyclin L1 and L2 interactions with CDK11 and splicing factors: influence of cyclin L isoforms on splice site selection. J Biol Chem 283, 7721–7732.

Lu H, Zawel L, Fisher L, Egly JM, Reinberg D. (1992). Human general transcription factor IIH phosphorylates the C-terminal domain of RNA polymerase II. Nature 358, 641–645.

McKinley KL, Cheeseman IM (2016). The molecular basis for centromere identity and function. Nat Rev Mol Cell Biol 17, 16–29.

Oka Y, Varmark H, Vitting-Seerup K, Beli P, Waage J, Hakobyan A, Mistrik M, Choudhary C, Rohde M, Bekker-Jensen S, *et al*. (2014). UBL5 is essential for pre-mRNA splicing and sister chromatid cohesion in human cells. EMBO Rep 15, 956–964.

Pak V, Eifler TT, Jager S, Krogan NJ, Fujinaga K, Peterlin BM (2015). CDK11 in TREX/THOC regulates HIV mRNA 3' end processing. Cell Host Microbe 18, 560–570.

Palozola KC, Donahue G, Liu H, Grant GR, Becker JS, Cote A, Yu H, Raj A, Zaret KS (2017). Mitotic transcription and waves of gene reactivation during mitotic exit. Science 358, 119–122.

Palozola KC, Liu H, Nicetto D, Zaret KS (2018). Low-level, global transcription during mitosis and dynamic gene reactivation during mitotic exit. Cold Spring Harb Symp Quant Biol 82,197–205.

Parsons GG, Spencer CA (1997). Mitotic repression of RNA polymerase II transcription is accompanied by release of transcription elongation complexes. Mol Cell Biol 17, 5791–5802.
Peng J, Zhu Y, Milton JT, Price DH (1998). Identification of multiple cyclin subunits of human P-TEFb. Genes Dev 12, 755–762.
Perea-Resa C, Bury L, Cheeseman IM, Blower MD (2020). Cohesin removal reprograms gene expression upon mitotic entry. Mol Cell 78, 127–140. e127.
Primorac I, Weir JR, Chiroli E, Gross F, Hoffmann I, van Gerwen S, Ciliberto A, Musacchio A (2013). Bub3 reads phosphorylated MELT repeats to promote spindle assembly checkpoint signaling. eLife 2, e01030.
Rakkaa T, Escude C, Giet R, Magnaghi-Jaulin L, Jaulin C (2014). CDK11(p58) kinase activity is required to protect sister chromatid cohesion at centromeres in mitosis. Chromosome Res 22, 267–276.
Schuh M, Lehner CF, Heidmann S (2007). Incorporation of Drosophila CID/CENP-A and CENP-C into centromeres during early embryonic anaphase. Curr Biol 17, 237–243.
Serizawa H, Makela TP, Conaway JW, Conaway RC, Weinberg RA, Young RA (1995). Association of Cdk-activating kinase subunits with transcription factor TFIIH. Nature 374, 280–282.
Spangler L, Wang X, Conaway JW, Conaway RC, Dvir A (2001). TFIIH action in transcription initiation and promoter escape requires distinct regions of downstream promoter DNA. Proc Natl Acad Sci USA 98, 5544–5549.
Sundaramoorthy S, Vazquez-Novelle MD, Lekomtsev S, Howell M, Petronczki M (2014). Functional genomics identifies a requirement of pre-mRNA splicing factors for sister chromatid cohesion. EMBO J 33, 2623–2642.
Takata H, Matsunaga S, Morimoto A, Ma N, Kurihara D, Ono-Maniwa R, Nakagawa M, Azuma T, Uchiyama S, Fukui K (2007). PHB2 protects sister-chromatid cohesion in mitosis. Curr Biol 17, 1356–1361.
Talbert PB, Henikoff S (2018). Transcribing centromeres: noncoding RNAs and kinetochore assembly. Trends Genet 34, 587–599.
Tang Z, Sun Y, Harley SE, Zou H, Yu H. (2004). Human Bub1 protects centromeric sister-chromatid cohesion through Shugoshin during mitosis. Proc Natl Acad Sci USA 101, 18012–18017.
Teves SS, An L, Bhargava-Shah A, Xie L, Darzacq X, Tjian R (2018). A stable mode of bookmarking by TBP recruits RNA polymerase II to mitotic chromosomes. eLife 7, e35621.
Trembley JH, Hu D, Hsu LC, Yeung CY, Slaughter C, Lahti JM, Kidd VJ (2002). PITSLRE p110 protein kinases associate with transcription complexes and affect their activity. J Biol Chem 277, 2589–2596.
Trembley JH, Hu DL, Slaughter CA, Lahti JM, Kidd VJ (2003). Casein kinase 2 interacts with cyclin-dependent kinase 11 (CDK11) in vivo and phosphorylates both the RNA polymerase II carboxyl-terminal domain and CDK11 in vitro. J Biol Chem 278, 2265–2270.
Valente ST, Gilmartin GM, Venkatarama K, Arriagada G, Goff SP (2009). HIV-1 mRNA 3′ end processing is distinctively regulated by eIF3f, CDK11, and splice factor 9G8. Mol Cell 36, 279–289.
van der Lelij P, Stocsits RR, Ladurner R, Petzold G, Kreidl E, Koch B, Schmitz J, Neumann B, Ellenberg J, Peters JM (2014). SNW1 enables sister chromatid cohesion by mediating the splicing of sororin and APC2 pre-mRNAs. EMBO J 33, 2643–2658.
Watrin E, Demidova M, Watrin T, Hu Z, Prigent C (2014). Sororin pre-mRNA splicing is required for proper sister chromatid cohesion in human cells. EMBO Rep 15, 948–955.
Williams SJ, Abrieu A, Losada A (2017). Bub1 targeting to centromeres is sufficient for Sgo1 recruitment in the absence of kinetochores. Chromosoma 126, 279–286.
Xiang J, Lahti JM, Grenet J, Easton J, Kidd VJ (1994). Molecular cloning and expression of alternatively spliced PITSLRE protein kinase isoforms. J Biol Chem 269, 15786–15794.
Yang L, Zhang Q, Niu T, Liu H (2021). SET levels contribute to cohesion fatigue. Mol Biol Cell 32, 1256–1266.
Zhang G, Lischetti T, Nilsson J (2014). A minimal number of MELT repeats supports all the functions of KNL1 in chromosome segregation. J Cell Sci 127, 871–884.
Zhou Y, Han C, Li D, Yu Z, Li F, Li F, An Q, Bai H, Zhang X, Duan Z, *et al*. (2015). Cyclin-dependent kinase 11(p110) (CDK11(p110)) is crucial for human breast cancer cell proliferation and growth. Sci Rep 5, 10433.